Reaction Dynamics of n-Heptane

Department of Aerospace and Mechanical Engineering

University of Notre Dame

Prepared by : Steven Brus

Prepared for : AME 48491 - Undergraduate Research

Dr. Joseph M. Powers

September 21, 2010

Contents

Abstract

This report considers a model of n-heptane combustion developed by Curran, et al. [1]. This model gives rise to reaction times scales four to five orders of magnitude faster than those predicted by molecular collision estimates. This is an indication of a deficiency in the reaction mechanism. The purpose of this study was to investigate the model in order to identify problem reactions and find a way to correct the time scale issue. Time scales for the individual reactions were calculated and used to create reduced models with physical initial and equilibrium time scales. Three different conditions were considered with initial temperatures of 850 K, 1175 K, and 1500 K. The full mechanism equilibrium time scales for these conditions were 1.5×10^{-15} s, 1.5×10^{-15} s, and 8.2×10^{-16} s, respectively. The reduced mechanisms had equilibrium time scales of 7.9×10^{-13} s, 1.2×10^{-12} s, and 1.3×10^{-12} s for each case. The reduced mechanisms were in good agreement with the full mechanism.

1   Introduction

Chemical kinetic reaction mechanisms play an important role in the study of hydrocarbon fuels. Today, hydrocarbon fuels are an essential source of energy used for transportation. Combustion models for these fuels are used to predict the performance of internal combustion engines. With these models, engines can be designed for improved efficiency and reduced emissions. One engine technology called Homogeneous Charge Compression Ignition (HCCI) has the potential to deliver the efficiency of a Diesel engine while maintaining the lower emissions of a gasoline engine [2]. However, the fuel ignition in these engines is difficult to control making accurate fuel combustion models a necessity for design improvements. n-Heptane is an important fuel being researched for this purpose due to its similarity to Diesel fuel and standard composition [3].

Chemical kinetic reaction mechanisms are comprised of systems of coupled nonlinear ordinary differential equations that describe the change in concentration of a species with respect to time. When these systems are linearized about a certain point, the local time scales of the reaction are given by the absolute value of the reciprocal of the eigenvalues of the local Jacobian matrix. Reaction mechanisms often involve a wide range of time scales making them what are known as stiff systems. The ratio of the slowest to the fastest time scale determines the stiffness of the reaction dynamics. The time scales of a reaction are important descriptors of its kinetics because they indicate the times when substantial species concentration changes occur. The n-heptane model [1] predicts very small time scales which will be shown to be on the order of 10^{-16} s. These are non-physical values because they are several orders of magnitude smaller than the predicted molecular collision times, the slowest of which are on the order of 10^{-11} s. Molecular collision times are the average amount of time between molecular collisions during a reaction [4]. Since chemical reactions are driven by inter-molecular collisions, no significant change in a species concentration can occur before these collision times. Finding the cause of these extremely small time scales is a useful way of identifying the problems with the current model which can lead to a more accurate way to simulate n-heptane combustion.

This report is organized as follows: the first section is an overview of HCCI technology and why the research of n-heptane is relevant to its advancement. Then the basic equations used to describe chemical reactions are presented followed by a discussion of molecular collision times. A

sample problem is then given as an example of reaction kinetics and time scale analysis for a system of reactions. The sections that follow describe the n-heptane model and the methodology used to create the reduced models with corrected time scales. Lastly conclusions are given.

2 HCCI Technology

HCCI engines operate by the auto-ignition of a compressed homogeneous mixture. Controlling the timing of the ignition creates a significant challenge which has limited HCCI engines to a narrow load operating range. Until this operating range is expanded, they are not practical for day to day consumer use especially at the lightest and highest loads. Neither today's gasoline nor Diesel engines create ignition timing problems because they are directly controlled. In a gasoline engine the combustion process is controlled by spark ignition used to ignite the fuel-air mixture at top-dead-center. Diesel engine ignition is also directly controlled by the injection of fuel into highly compressed air at top-dead-center causing combustion to occur at the fuel-air boundary. The only way to control HCCI combustion is via the pressure and temperature conditions in the cylinder when the intake valve closes. Therefore it is critical to have an accurate model for the reaction dynamics of the fuel.

HCCI engines have the potential to significantly reduce nitrogen oxide, or NO_x, emissions while improving fuel economy up to 15-20% over conventional spark ignition engines [2]. NO_x refers to the chemical compounds NO and NO_2. Both are harmful air pollutants that have negative environmental and public health effects. HCCI engines are able to combine the high efficiency of a Diesel engine with the lower emissions of gasoline engines. HCCI engines can be adapted to run on multiple types of hydrocarbon fuels, most importantly gasoline and Diesel. These engines burn fuel at a reduced temperature, which is advantageous for eliminating NO_x in the exhaust. Additionally, the homogeneous nature of the fuel-air mixture during combustion greatly reduces particulate matter emissions. These engines can be operated with lean mixtures, allowing the engine to run unthrottled and at lower temperatures. This reduces both the pumping work required as well as the closed-cycle heat losses [2]. These factors increase the efficiency of HCCI engines to that of a Diesel engine.

In order to overcome the difficulties created by auto-ignition, the combustion process must

be better modeled. Due to the complexities of distillate fuels such as gasoline or Diesel, it is not useful to use these fuels for reaction mechanisms. These fuels have a broad range of hydrocarbon constituents which vary depending on the sample [3]. Therefore, surrogate fuels with standard compositions such as n-heptane and iso-octane are most often used in detailed combustion models. n-Heptane is a widely researched hydrocarbon with a chemical formula of $H_3C(CH_2)_5CH_3$ or C_7H_{16}. It is a primary reference fuel and relevant to HCCI research because it is a Diesel surrogate. An important characteristic of n-heptane combustion is its negative temperature coefficient (NTC) behavior. Throughout most of the combustion process fuel consumption increases with temperature, while in the NTC region fuel consumption decreases as the temperature rises. As a result of this NTC region, two explosions occur under some conditions. n-Heptane fuel is the zero point on the octane rating scale and is also used to study knock in spark ignition engines which is caused by the same phenomenon as HCCI ignition. Better understanding n-heptane oxidation is important to realizing the potential advantages of HCCI engines.

3 Reaction Kinetics

3.1 Single Reaction

To give a background on reaction kinetics, consider an isothermal, isochoric system and the following reversible reaction:

$$\sum_{i=1}^{N} \nu_i' \chi_i \rightleftharpoons \sum_{i=1}^{N} \nu_i'' \chi_i, \tag{1}$$

where χ_i is the ith chemical species, $i = 1, \ldots, N$, and ν_i' and ν_i'' are the forward and reverse stoichiometric coefficients. The net stoichiometric coefficient for each species, ν_i is defined as

$$\nu_i = \nu_i'' - \nu_i'. \tag{2}$$

Continuum kinetics models the evolution of species concentration i, $\overline{\rho}_i$, during the reaction by the differential equation:

$$\frac{d\overline{\rho}_i}{dt} = \nu_i a T^\beta \exp\left(\frac{-\overline{E}}{\overline{R}T}\right) \left(\prod_{k=1}^{N} \overline{\rho}_k^{\nu_k'}\right) \left(1 - \frac{1}{K_c} \prod_{k=1}^{N} \overline{\rho}_k^{\nu_k}\right), \tag{3}$$

where T is the temperature, $\overline{R}$ is the universal gas constant, a is collision frequency factor, β is the temperature-dependency exponent, and $\overline{E}$ is the activation energy. The equilibrium constant K_c for the reaction is

$$K_c = \exp\left(\frac{-\Delta G^o}{\overline{R}T}\right). \tag{4}$$

It is common to define the following term, $k(T)$, from Equation (3) which is often referred to as the Arrhenius rate,

$$k(T) \equiv \nu_i a T^\beta \exp\left(\frac{-\overline{E}}{\overline{R}T}\right). \tag{5}$$

In Equation (3), the product of all $\overline{\rho}_k^{\nu_k'}$ corresponds to the forward reaction while the product of all $\overline{\rho}_k^{\nu_k}$ multiplied by $1/K_c$ describes the reverse reaction. Together these represent the law of mass action for the reaction. Defining the reaction rate, r, to be

$$r \equiv a T^\beta \exp\left(\frac{-\overline{E}}{\overline{R}T}\right) \left(\prod_{k=1}^{N} \overline{\rho}_k^{\nu_k'}\right) \left(1 - \frac{1}{K_c} \prod_{k=1}^{N} \overline{\rho}_k^{\nu_k}\right), \tag{6}$$

allows Equation (3) to be written in a simpler form:

$$\frac{d\overline{\rho}_i}{dt} = \nu_i r. \tag{7}$$

3.2   Extension for Systems of Reactions

Reaction mechanisms consist of multiple reactions so the equations from the previous section must be extended for these systems. A reaction mechanism with $j = 1, \ldots, J$, reactions can be repre-

sented as

$$\sum_{i=1}^{N} \nu'_{ij}\chi_i \rightleftharpoons \sum_{i=1}^{N} \nu''_{ij}\chi_i. \tag{8}$$

Now the evolution of spices i for $i = 1, \ldots, N$ due to the all of the reactions is

$$\frac{d\overline{\rho}_i}{dt} = \sum_{j=1}^{J} \nu_{ij} a_j T^{\beta_j} \exp\left(\frac{-\overline{E}_j}{\overline{R}T}\right) \left(\prod_{k=1}^{N} \overline{\rho}_k^{\nu'_{kj}}\right) \left(1 - \frac{1}{K_c} \prod_{k=1}^{N} \overline{\rho}_{kj}^{\nu_k}\right), \tag{9}$$

$$\frac{d\overline{\rho}_i}{dt} = \sum_{j=1}^{J} \nu_{ij} r_j. \tag{10}$$

The equilibrium constant for each of the J reactions is

$$K_{c,j} = \exp\left(\frac{-\Delta G_j^o}{\overline{R}T}\right). \tag{11}$$

In vector notation a reaction mechanism can be represented as

$$\frac{d\overline{\boldsymbol{\rho}}}{dt} = \boldsymbol{\nu} \cdot \mathbf{r}, \tag{12}$$

where $\overline{\boldsymbol{\rho}}$ is a column vector of dimension $N \times 1$, $\boldsymbol{\nu}$ is a rectangular matrix of dimension $N \times J$, and $\mathbf{r}$ is a column vector of dimension $J \times 1$.

3.3   Energy Conservation

The equations given in Sections 3.1 and 3.2 apply to isothermal cases. Since most of the calculations done with the model are non-isothermal, the first law of thermodynamics must be used in order to consider adiabatic isochoric and isobaric reactions. Using energy conservation, an expression for the rate of temperature change with respect to time can be found. The next two sections summarize the energy conservation discussion in Reference [5].

3.3.1 Adiabatic, Isochoric Reaction

The differential form of the first law of thermodynamics is

$$\frac{du}{dt} = \frac{\delta q}{dt} - \frac{\delta w}{dt} = 0, \tag{13}$$

where u is the internal energy per unit mass, q is the heat transfer per unit mass, and w is the work per unit mass. Here the notation δ denotes an inexact differential. Since there is no heat transfer, $\delta q/dt = 0$, and because the volume is constant, $\delta w/dt = 0$. Therefore, Equation (13) becomes

$$\frac{du}{dt} = 0. \tag{14}$$

The internal energy of the mixture is given by

$$u = \sum_{i=1}^{N} u_i Y_i. \tag{15}$$

In Equation (15), u_i is the internal energy of species i, and Y_i is the mass faction of species i, given by

$$Y_i = \frac{m_i}{m_o} = \frac{\overline{\rho}_i M_i}{\rho}, \tag{16}$$

where m_i and M_i are the mass and molecular mass of the ith species, $m_o = \sum_{i=1}^{N} m_i$ is the total mixture mass, and $\rho = m_o/V$ is the mixture density. Differentiating Equation (15) and substituting into Equation (14) gives

$$\frac{du}{dt} = \sum_{i=1}^{N} Y_i \frac{du_i}{dt} + \sum_{i=1}^{N} u_i \frac{dY_i}{dt} = 0. \tag{17}$$

Because the mixture is assumed to be composed of ideal gases, the internal energy and specific heat at constant volume, c_{vi}, for each of the i spaces are functions temperature only. This means the specific heat at constant volume is defined as

$$c_{vi} = \frac{du_i}{dT}, \tag{18}$$

and it follows that

$$\frac{du_i}{dt} = c_{vi}\frac{dT}{dt}. \tag{19}$$

Substituting Equation (19) into Equation (17) gives

$$\frac{du}{dt} = \sum_{i=1}^{N} c_{vi}Y_i\frac{dT}{dt} + \sum_{i=1}^{N} u_i\frac{dY_i}{dt} = 0. \tag{20}$$

Since the specific heat for the mixture is defined as

$$c_v = \sum_{i=1}^{N} c_{vi}Y_i, \tag{21}$$

Equation (20) can be written as,

$$\frac{du}{dt} = c_v\frac{dT}{dt} + \sum_{i=1}^{N} u_i\frac{dY_i}{dt} = 0. \tag{22}$$

Using Equation (16) and Equation (7), an expression for dY_i/dt can be found

$$\frac{dY_i}{dt} = \frac{\nu_i r_i M_i}{\rho}. \tag{23}$$

Substituting Equation (23) into Equation (22) and rearranging to find dT/dt gives

$$\frac{dT}{dt} = -\frac{1}{\rho c_v}\sum_{i=1}^{N} u_i\nu_i r_i M_i. \tag{24}$$

3.3.2 Adiabatic, Isobaric Reaction

Since for these conditions $\delta q/dt = 0$ and $\delta w/dt = Pdv/dt$, where v is the specific volume of the mixture and P is the pressure, the differential form of the first law from Equation (13) can be written as

$$\frac{du}{dt} + P\frac{dv}{dt} = 0. \tag{25}$$

The enthalpy of the mixture per unit mass, h, is given by

$$h = u + Pv. \tag{26}$$

Differentiating Equation (26) gives

$$\frac{dh}{dt} = \frac{du}{dt} + P\frac{dv}{dt} + v\frac{dP}{dt} = 0. \tag{27}$$

Using Equation (25) and realizing $dP/dt = 0$ because the pressure is constant means the enthalpy is constant during the reaction. The enthalpy per unit mass for the mixture is given by

$$h = \sum_{i=1}^{N} h_i Y_i, \tag{28}$$

where h_i is the enthalpy per unit mass of the ith species. Differentiating Equation (28) and substituting into Equation (27) gives

$$\frac{dh}{dt} = \sum_{i=1}^{N} Y_i \frac{dh_i}{dt} + \sum_{i=1}^{N} h_i \frac{dY_i}{dt} = 0. \tag{29}$$

For ideal gases, the specific heat at constant pressure for the ith spaces is defined as

$$c_{pi} = \frac{dh_i}{dT}. \tag{30}$$

Therefore,

$$\frac{dh_i}{dt} = c_{pi}\frac{dT}{dt}. \tag{31}$$

Substituting Equation (31) into Equation(29) gives

$$\frac{dh}{dt} = \sum_{i=1}^{N} c_{pi} Y_i \frac{dT}{dt} + \sum_{i=1}^{N} h_i \frac{dY_i}{dt} = 0. \tag{32}$$

Since the specific heat at constant pressure for the mixture is defined as

$$c_p = \sum_{i=1}^{N} c_{pi} Y_i, \tag{33}$$

Equation (32) can be written as

$$\frac{dh}{dt} = c_p \frac{dT}{dt} + \sum_{i=1}^{N} h_i \frac{dY_i}{dt} = 0. \tag{34}$$

Finally, substituting Equation (23) and solving for dT/dt gives

$$\frac{dT}{dt} = -\frac{1}{\rho c_p} \sum_{i=1}^{N} h_i \nu_i r_i M_i. \tag{35}$$

4   Molecular Collision Times

The parameter used to determine the physicality of the n-heptane mechanism time scales is the molecular collision time, t_c, which is the average time between molecular collisions. To develop the equations to estimate this value, consider the simplest molecular model in kinetic theory called the "billiard ball" model [4]. This model assumes molecules are structureless, perfectly elastic spheres. There are no attractive forces between each molecule and repulsive forces only during contact. The information necessary to describe this model are the mass, diameter, speed, and number of molecules per unit volume for each type of molecule. An important concept in determining the collision times between molecules is the mean free path. The mean free path is the average distance a molecule travels between collisions. Once this average distance has been determined and the speed of a molecule is known, the molecular collision time may be found by dividing the mean free path by the molecule's velocity.

The following summary of the derivation for the mean free path has been adapted from [4]. Assume a billiard ball model where all molecules are of one species and have the same diameter d with n molecules per unit volume. Because collisions occur when one molecule reaches a distance d from the center of another, each molecule has associated with it a "sphere of influence" of radius d. If one molecule is assumed to be traveling at a constant velocity equal to the mean molecular speed $\overline{C}$ while all the others are standing still, the volume swept out by the sphere of influence per

10

unit time is $\pi d^2 \overline{C}$. Therefore the number of centers lying in this volume will be $\pi d^2 \overline{C} n$. Each time a center of another molecule lies in the volume swept out by the sphere of influence, a collision will occur. This means the number of collisions per unit time, Θ, for the molecule is

$$\Theta = \pi d^2 \overline{C} n. \tag{36}$$

In terms of mass density, defined as $\rho = mn$ where m is the mass of the molecules, Equation (36) can be written as

$$\Theta = \pi d^2 \overline{C} \frac{\rho}{m}. \tag{37}$$

Since the distance traveled by the molecule per unit time is $\overline{C}$, the mean free path, λ, can be found by dividing this distance by the number of collisions per unit time from Equation (37)

$$\lambda = \frac{\overline{C}}{\Theta} = \frac{m}{\pi d^2 \rho}. \tag{38}$$

In order to account for the motion of the other molecules, the mean relative speed of the molecules, which can be shown to be $\overline{C}\sqrt{2}$, should be used in Equation (37). With this correction the final expression for the mean free path is

$$\lambda = \frac{m}{\sqrt{2}\pi d^2 \rho}. \tag{39}$$

Therefore the average time between collisions for a given molecule with a velocity $\overline{C}$ is

$$t_c = \frac{\lambda}{\overline{C}} = \frac{m}{\sqrt{2}\pi d^2 \rho \overline{C}}. \tag{40}$$

Equation (40) assumes all molecules are identical which is not the case in an n-heptane reaction. Therefore, each species has a different collision time associated with it, and Equation (40) must take into account the presence of different species. For the n-heptane mechanism, the fastest collision times are on the order of 10^{-13} s, and the slowest are on the order of 10^{-11} s. Therefore, these are the benchmarks for the time scales of the mechanism.

The calculation for the molecular collision time estimate of a hydrogen atom at the beginning of an n-heptane reaction will be shown as an example. The velocity of the molecule will be taken to be the mixture sound speed given by

$$\overline{C}^2 = \gamma RT, \tag{41}$$

where γ is the ratio of the mixture specific heats c_p/c_v. For a stoichiometric mixture and initial conditions of $T = 850 \ K$ and $P = 30 \ atm$, $c_p = 1.195 \times 10^7 \ erg/(g \ K)$ and $c_v = 9.135 \times 10^5 \ erg/(g \ K)$. Therefore from Equation (41), $\overline{C} = 5.596 \times 10^4 \ cm/s$. The initial density is given by the ideal gas law

$$\rho = \frac{P}{\overline{R}T} = 1.27 \times 10^{-2} \ g/cm^3. \tag{42}$$

The mass of a hydrogen atom is $1.674 \times 10^{-24} \ g$ and the diameter is $2.050 \times 10^{-8} \ cm$ [6]. Using these values in Equation (40) gives an estimated collision time of $t_c = 1.261 \times 10^{-12} \ s$.

5   Sample Problem

As a simple example of how the reaction kinetics equations given in Section 3.1 are applied to a system of reactions, consider a reaction system known as the Zel'dovich mechanism. This reaction system describes the production of NO, which is a pollutant resulting from high temperature combustion. In automotive engine design, NO is important from an emissions standpoint and is one of the reasons the lower temperature combustion of an HCCI engine is desirable. The problem considered will be similar to that found in a paper by Al-Khateeb et al. [7]. The reactions and Arrhenius coefficients are given in Table 1.

Table 1: Zel'dovich mechanism

j	Reaction	a_j $[cm^3/(mol \ s \ K_j^\beta)]$	β_j	$\overline{E}_j$ $[cal/mol]$
1	$N + NO \rightleftharpoons N_2 + O$	2.1077×10^{13}	0.00	0.0
2	$N + NO_2 \rightleftharpoons NO + O$	5.841×10^9	1.01	6195.6

5.1 Kinetics

There are five species in this mechanism, whose concentrations are represented in vector notation as

$$\overline{\rho} = \begin{pmatrix} \overline{\rho}_{NO} \\ \overline{\rho}_N \\ \overline{\rho}_{N_2} \\ \overline{\rho}_O \\ \overline{\rho}_{O_2} \end{pmatrix}. \tag{43}$$

Using Equation (6), the reaction rates for the system of two reactions in vector notation are

$$\mathbf{r} = \begin{pmatrix} r_1 \\ r_2 \end{pmatrix} = \begin{pmatrix} a_1 T^{\beta_1} \exp\left(\frac{-\overline{E}_1}{RT}\right) \left(\overline{\rho}_N \overline{\rho}_{NO} - \frac{1}{K_{c,1}} \overline{\rho}_{N_2} \overline{\rho}_O\right) \\ a_2 T^{\beta_2} \exp\left(\frac{-\overline{E}_2}{RT}\right) \left(\overline{\rho}_N \overline{\rho}_{O_2} - \frac{1}{K_{c,2}} \overline{\rho}_{NO} \overline{\rho}_O\right) \end{pmatrix}. \tag{44}$$

Substituting into Equation (12), the system becomes

$$\frac{d}{dt} \begin{pmatrix} \overline{\rho}_{NO} \\ \overline{\rho}_N \\ \overline{\rho}_{N_2} \\ \overline{\rho}_O \\ \overline{\rho}_{O_2} \end{pmatrix} = \begin{pmatrix} -1 & 1 \\ -1 & -1 \\ 1 & 0 \\ 1 & 1 \\ 0 & -1 \end{pmatrix} \begin{pmatrix} r_1 \\ r_2 \end{pmatrix}. \tag{45}$$

This system can be row reduced to upper triangular form to remove the linear constraints.

$$\text{Add row 1 to row 4}: \quad \frac{d}{dt} \begin{pmatrix} \overline{\rho}_{NO} \\ \overline{\rho}_N \\ \overline{\rho}_{N_2} \\ \overline{\rho}_O + \overline{\rho}_{NO} \\ \overline{\rho}_{O_2} \end{pmatrix} = \begin{pmatrix} -1 & 1 \\ -1 & -1 \\ 1 & 0 \\ 0 & 2 \\ 0 & -1 \end{pmatrix} \begin{pmatrix} r_1 \\ r_2 \end{pmatrix}. \tag{46}$$

$$\text{Add row 1 to row 3}: \quad \frac{d}{dt} \begin{pmatrix} \overline{\rho}_{NO} \\ \overline{\rho}_{N} \\ \overline{\rho}_{N_2} + \overline{\rho}_{NO} \\ \overline{\rho}_{O} + \overline{\rho}_{NO} \\ \overline{\rho}_{O_2} \end{pmatrix} = \begin{pmatrix} -1 & 1 \\ -1 & -1 \\ 0 & 1 \\ 0 & 2 \\ 0 & -1 \end{pmatrix} \begin{pmatrix} r_1 \\ r_2 \end{pmatrix}. \tag{47}$$

$$\text{Subtract row 1 from row 2}: \quad \frac{d}{dt} \begin{pmatrix} \overline{\rho}_{NO} \\ \overline{\rho}_{N} - \overline{\rho}_{NO} \\ \overline{\rho}_{N_2} + \overline{\rho}_{NO} \\ \overline{\rho}_{O} + \overline{\rho}_{NO} \\ \overline{\rho}_{O_2} \end{pmatrix} = \begin{pmatrix} -1 & 1 \\ 0 & -2 \\ 0 & 1 \\ 0 & 2 \\ 0 & -1 \end{pmatrix} \begin{pmatrix} r_1 \\ r_2 \end{pmatrix}. \tag{48}$$

$$\text{Add row 2 to } -2 \times \text{row 5}: \quad \frac{d}{dt} \begin{pmatrix} \overline{\rho}_{NO} \\ \overline{\rho}_{N} - \overline{\rho}_{NO} \\ \overline{\rho}_{N_2} + \overline{\rho}_{NO} \\ \overline{\rho}_{O} + \overline{\rho}_{NO} \\ -2\overline{\rho}_{O_2} + \overline{\rho}_{N} - \overline{\rho}_{NO} \end{pmatrix} = \begin{pmatrix} -1 & 1 \\ 0 & -2 \\ 0 & 1 \\ 0 & 2 \\ 0 & 0 \end{pmatrix} \begin{pmatrix} r_1 \\ r_2 \end{pmatrix}. \tag{49}$$

$$\text{Add row 2 to row 4}: \quad \frac{d}{dt} \begin{pmatrix} \overline{\rho}_{NO} \\ \overline{\rho}_{N} - \overline{\rho}_{NO} \\ \overline{\rho}_{N_2} + \overline{\rho}_{NO} \\ \overline{\rho}_{O} + \overline{\rho}_{N} \\ -2\overline{\rho}_{O_2} + \overline{\rho}_{N} - \overline{\rho}_{NO} \end{pmatrix} = \begin{pmatrix} -1 & 1 \\ 0 & -2 \\ 0 & 1 \\ 0 & 0 \\ 0 & 0 \end{pmatrix} \begin{pmatrix} r_1 \\ r_2 \end{pmatrix}. \tag{50}$$

$$\text{Add row 2 to } 2 \times \text{row 3}: \quad \frac{d}{dt} \begin{pmatrix} \overline{\rho}_{NO} \\ \overline{\rho}_N - \overline{\rho}_{NO} \\ 2\overline{\rho}_{N_2} + \overline{\rho}_{NO} + \overline{\rho}_N \\ \overline{\rho}_O + \overline{\rho}_N \\ -2\overline{\rho}_{O_2} + \overline{\rho}_N - \overline{\rho}_{NO} \end{pmatrix} = \begin{pmatrix} -1 & 1 \\ 0 & -2 \\ 0 & 0 \\ 0 & 0 \\ 0 & 0 \end{pmatrix} \begin{pmatrix} r_1 \\ r_2 \end{pmatrix}. \tag{51}$$

The form of Equation (51) reveals the free variables to be $\overline{\rho}_{NO}$ and $\overline{\rho}_N$. The bottom three equations of Equation (51) can be integrated to give the constraint equations to express the free variables in terms of the others. Integrating these equations gives

$$\overline{\rho}_{NO} + \overline{\rho}_N + 2\overline{\rho}_{N_2} = C_1, \tag{52}$$

$$\overline{\rho}_N + \overline{\rho}_O = C_2, \tag{53}$$

$$\overline{\rho}_{NO} - \overline{\rho}_N + 2\overline{\rho}_{O_2} = C_3. \tag{54}$$

Therefore, in terms of the free variables,

$$\begin{pmatrix} \overline{\rho}_{N_2} \\ \overline{\rho}_O \\ \overline{\rho}_{O_2} \end{pmatrix} = \begin{pmatrix} \frac{1}{2}C_1 - \frac{1}{2}\overline{\rho}_{NO} - \frac{1}{2}\overline{\rho}_N \\ C_2 - \overline{\rho}_N \\ \frac{1}{2}C_3 - \frac{1}{2}\overline{\rho}_{NO} + \frac{1}{2}\overline{\rho}_N \end{pmatrix}. \tag{55}$$

Substituting Equation (55) into (44), the reaction rate vector becomes

$$\begin{pmatrix} r_1 \\ r_2 \end{pmatrix} = \begin{pmatrix} k_1 \left(\overline{\rho}_N \overline{\rho}_{NO} - \frac{1}{K_{c,1}} \left(\frac{1}{2}C_1 - \frac{1}{2}\overline{\rho}_{NO} - \frac{1}{2}\overline{\rho}_N \right) (C_2 - \overline{\rho}_N) \right) \\ k_2 \left(\overline{\rho}_N \left(\frac{1}{2}C_3 - \frac{1}{2}\overline{\rho}_{NO} + \overline{\rho}_N \right) - \frac{1}{K_{c,2}}\overline{\rho}_{NO}(C_2 - \overline{\rho}_N) \right) \end{pmatrix}. \tag{56}$$

Now the reaction mechanism has been reduced to a system of two differential equations in two unknowns

$$\frac{d}{dt} \begin{pmatrix} \overline{\rho}_{NO} \\ \overline{\rho}_N \end{pmatrix} = \begin{pmatrix} -1 & 1 \\ 0 & -2 \end{pmatrix} \begin{pmatrix} r_1 \\ r_2 \end{pmatrix}. \tag{57}$$

15
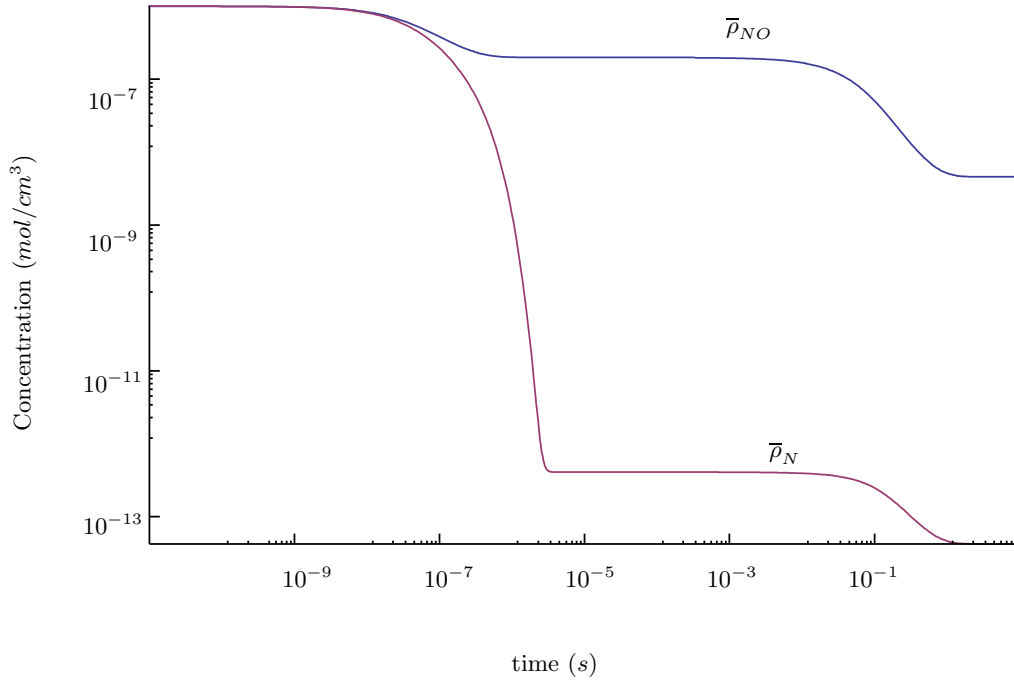
Figure 1: Species concentration vs. time for N and NO

The solution to this problem at a temperature of 1500 K and initial concentrations for all species of 1×10^{-6} mol/cm^3 can be seen in Figure 1. The equilibrium conditions for each species are found by finding the roots to Equation (57) when the right hand side is set equal to 0:

$$\begin{pmatrix} 0 \\ 0 \end{pmatrix} = \begin{pmatrix} -1 & 1 \\ 0 & -2 \end{pmatrix} \begin{pmatrix} r_1 \\ r_2 \end{pmatrix}. \tag{58}$$

The only physical root of this system is $(\overline{\rho}_{NO}, \overline{\rho}_N) = (4.597 \times 10^{-9}, 4.231 \times 10^{-14})$ mol/cm^3.

5.2 Eigenvalues and Time Scales

To investigate the time scales of the reaction system at the initial and equilibrium states, the differential equations will need to be locally linearized. Equation (57) can be expressed as

$$\frac{d}{dt} \begin{pmatrix} \overline{\rho}_{NO} \\ \overline{\rho}_N \end{pmatrix} = \begin{pmatrix} f_{NO}(\overline{\rho}_{NO}, \overline{\rho}_N) \\ f_N(\overline{\rho}_{NO}, \overline{\rho}_N) \end{pmatrix}. \tag{59}$$

16

The Taylor series expansion of Equation (59) in the neighborhood of equilibrium is

$$\frac{d}{dt}(\overline{\rho}_{NO} - \overline{\rho}_{NO}^e) = f_{NO}|_e + \frac{\partial f_{NO}}{\partial \overline{\rho}_{NO}}\bigg|_e (\overline{\rho}_{NO} - \overline{\rho}_{NO}^e) + \frac{\partial f_{NO}}{\partial \overline{\rho}_N}\bigg|_e (\overline{\rho}_N - \overline{\rho}_N^e) + \ldots, \qquad (60)$$

$$\frac{d}{dt}(\overline{\rho}_N - \overline{\rho}_N^e) = f_N|_e + \frac{\partial f_N}{\partial \overline{\rho}_{NO}}\bigg|_e (\overline{\rho}_{NO} - \overline{\rho}_{NO}^e) + \frac{\partial f_N}{\partial \overline{\rho}_N}\bigg|_e (\overline{\rho}_N - \overline{\rho}_N^e) + \ldots, \qquad (61)$$

where $\overline{\rho}_{NO}^e$ and $\overline{\rho}_N^e$ are the equilibrium concentrations. Evaluating the terms in Equation (61) gives

$$f_{NO}|_e = 0,$$

$$\frac{\partial f_{NO}}{\partial \overline{\rho}_{NO}}\bigg|_e = \left(\frac{1}{K_{c,1}} - \frac{k_1}{2} + \frac{k_2}{K_{c,2}} - \frac{k_2}{2}\right)\overline{\rho}_N^e - \left(\frac{k_1 C_2}{2K_{c,1}} + \frac{k_2 C_2}{K_{c,2}}\right),$$

$$\frac{\partial f_{NO}}{\partial \overline{\rho}_N}\bigg|_e = \left(\frac{k_1}{2K_{c,1}} - k_1 + \frac{k_2}{K_{c,2}} - \frac{k_2}{2}\right)\overline{\rho}_{NO}^e + \left(\frac{k_1}{K_{c,1}} + k_2\right)\overline{\rho}_N^e + \left(\frac{k_2 C_3}{2} - \frac{k_1(C_1 + C_2)}{2K_{c,1}}\right),$$

$$f_N|_e = 0,$$

$$\frac{\partial f_N}{\partial \overline{\rho}_{NO}}\bigg|_e = \left(\frac{k_1}{2K_{c,1}} - k_1 + \frac{k_2}{2} - \frac{k_2}{K_{c,2}}\right)\overline{\rho}_N^e + \left(\frac{k_2 C_2}{K_{c,2}} - \frac{k_1 C_2}{2K_{c,1}}\right),$$

$$\frac{\partial f_N}{\partial \overline{\rho}_N}\bigg|_e = \left(\frac{k_1}{2K_{c,1}} - k_1 + \frac{k_2}{2} - \frac{k_2}{K_{c,2}}\right)\overline{\rho}_{NO}^e + \left(\frac{k_1}{K_{c,1}} - k_2\right)\overline{\rho}_N^e - \left(\frac{k_2(C_1 + C_2)}{2K_{c,1}} + \frac{k_2 C_3}{2}\right).$$

Now the linearized system becomes

$$\frac{d}{dt}\begin{pmatrix} \overline{\rho}_{NO} - \overline{\rho}_{NO}^e \\ \overline{\rho}_N - \overline{\rho}_N^e \end{pmatrix} = \begin{pmatrix} \frac{\partial f_{NO}}{\partial \overline{\rho}_{NO}}\big|_e & \frac{\partial f_{NO}}{\partial \overline{\rho}_N}\big|_e \\ \frac{\partial f_N}{\partial \overline{\rho}_{NO}}\big|_e & \frac{\partial f_N}{\partial \overline{\rho}_N}\big|_e \end{pmatrix}\begin{pmatrix} \overline{\rho}_{NO} - \overline{\rho}_{NO}^e \\ \overline{\rho}_N - \overline{\rho}_N^e \end{pmatrix}. \qquad (62)$$

Finding the eigenvalues of this Jacobian matrix will give the time scales of the reaction near equilibrium. The eigenvalues are found from solving the characteristic polynomial from the equation

$$\begin{vmatrix} \frac{\partial f_{NO}}{\partial \overline{\rho}_{NO}}\big|_e - \lambda & \frac{\partial f_{NO}}{\partial \overline{\rho}_N}\big|_e \\ \frac{\partial f_N}{\partial \overline{\rho}_{NO}}\big|_e & \frac{\partial f_N}{\partial \overline{\rho}_N}\big|_e - \lambda \end{vmatrix} = 0. \qquad (63)$$

Once the eigenvalues have been found, the time scales are given by

$$\tau_i = \frac{1}{|\lambda_i|}. \qquad (64)$$

17

After substituting values for the problem, the linear system is

$$\frac{d}{dt}\begin{pmatrix} \bar{\rho}_{NO} - 4.597 \times 10^{-9} \\ \bar{\rho}_N - 4.231 \times 10^{-14} \end{pmatrix} = \begin{pmatrix} -1.173 \times 10^1 & 1.078 \times 10^6 \\ 9.943 \times 10^0 & -1.271 \times 10^6 \end{pmatrix} \begin{pmatrix} \bar{\rho}_{NO} - 4.597 \times 10^{-9} \\ \bar{\rho}_N - 4.231 \times 10^{-14} \end{pmatrix}. \quad (65)$$

Solving Equation (63) to find the eigenvalues and substituting into Equation (64) gives equilibrium time scales of

$$\tau_{1_e} = 7.865 \times 10^{-7} \ s, \quad (66)$$

$$\tau_{2_e} = 3.031 \times 10^{-1} \ s. \quad (67)$$

Similarly, evaluating the Jacobian matrix at the initial conditions and finding the eigenvalues gives initial time scales of

$$\tau_{1_i} = 2.373 \times 10^{-8} \ s, \quad (68)$$

$$\tau_{2_i} = 4.247 \times 10^{-7} \ s. \quad (69)$$

The relevance of the equilibrium time scales can be seen in Figure 1. The first significant change in species concentration occurs in the neighborhood of τ_{1_e} and another significant change occurs in the neighborhood of τ_{2_e}. This shows why time scales faster than molecular collision times are non-physical. They correspond to species concentration changes that occur too fast to be caused by collisions. Without the occurrence of collisions between molecules the system cannot react. Time scales that indicate concentration changes have occurred before collisions take place point to a problem in the model for the reaction.

6   Modeling of n-Heptane

The n-heptane mechanism investigated here was created by the authors of Reference [1]. The model is extensive, considering 561 chemical species and 2538 reversible reactions. The first step taken in analyzing the mechanism was to compare its predictions to those from the literature. Comparisons were made with both experimental and computational results from References [3] and [8]. This

verified that further analysis would be performed with the correct model and properly configured code. The next step was to calculate the initial and final time scales for each individual reaction. These results were sorted by increasing initial time scale to identify problem reactions. Once the reactions with the fastest time scales were known, they were removed one by one, fastest to slowest from the mechanism until both the initial and equilibrium time scales for the reaction were physical. Once this was achieved, the reduced mechanisms were compared to the full mechanism to investigate the effect reaction removal had on the dynamics of the reaction.

6.1   Kinetics Model

The n-heptane model of Reference [1] was designed to encompass a complete range of temperatures and pressures of common n-heptane combustion. The mechanism was created beginning with small hydrocarbons and progressively adding larger ones. The authors compared the mechanism predictions to experimental data from studies done in variable pressure flow reactors, jet-stirred reactors, shock tubes, and rapid compression machines. An important goal of Reference [1] was to correctly model the NTC region across the entire range of conditions. Additionally, a sensitivity study was performed to identify the types of reactions have the greatest effect on the overall oxidation process. While many classes of reactions where found to be critical to the mechanism, others were determined be not important.

6.2   Computational Model

The program used to test the n-heptane model preforms the integration of the reaction mechanism ODE's and calculates the equilibrium conditions. The ODE solver used is called LSODE [9], and an implicit integration method was used for all calculations. The program utilizes the CHEMKIN Chemical Kinetics Package [6] to provide data for the calculations. Species are assumed to have calorically imperfect, ideal gas behavior. The code can be configured for four combinations of adiabatic, isothermal, isobaric and isochoric conditions.

The feature of the program most relevant to this work is its inclusion of IMSL [10] subroutines which compute the eigenvalues of the system. The eigenvalue calculator used is a double precision subroutine called DEVLRG. DEVLRG computes all of the eigenvalues of a real matrix. The first step in doing this is to balance the matrix. Balancing reduces the sensitivity of the eigenvalues to

roundoff errors. Since these errors are generally proportional to the Euclidean norm of the matrix, or the square root of the sum of the squares of the matrix elements, balancing is a way to reduce the overall norm of the matrix without changing the eigenvalues. This is done through similarity transformations that make the norms of corresponding rows and columns more uniform. The balanced matrix is then reduced to upper Hessenberg form. This means it has all zero entries below the first sub-diagonal. The reduction is done through Gauss similarity transformations with partial pivoting. The eigenvalues are then computed using a hybrid double-shifted LR-QR algorithm. The QR algorithm maintains upper Hessenberg form and reduces the number of iterations necessary for convergence. More information on the algorithm can be found in Reference [11]. In the code, this subroutine is typically used to compute eigenvalues at the initial and equilibrium states but can calculate them at each time step of the integration.

6.3 Model Comparisons

6.3.1 Experimental Comparison

To begin analyzing the n-heptane reaction mechanism, the model was first used to repeat the results of a shock tube study preformed by Gauthier et al. [3]. The study measured the ignition time delay for n-heptane in low pressure shock tubes. The data was intended to provide a standard for validating and improving reaction mechanisms under HCCI conditions [3]. To repeat the measurements, the n-heptane reaction mechanism was run under isobaric, adiabatic conditions. The initial fuel-air mixture had a stoichiometric equivalence ratio, $\phi = 1$. The ignition delay was measured by locating the inflection point in the temperature vs. time plot. The results of the comparison can be seen in Table 2. The ignition delays from the model agree fairly well with the measured delays from the study, especially at the higher pressures. A plot showing some of the species concentrations and temperature vs. time for $T_i = 1344\ K$ is shown in Figure 2.

6.3.2 Computational Comparison

The predictions of the model were also compared to those found by Lu et al. [8]. The authors use the same detailed n-heptane reaction mechanism considered here to develop a smaller, non-stiff mechanism. The authors also predict very small time scales on the order of $10^{-3}\ ns$ in the full

Table 2: Ignition Delay Comparison

Initial Temperature (K)	Pressure (atm)	τ_{ign} from [3] (μs)	τ_{ign} from Model (μs)
1249	1.97	529	774
1299	1.89	311	403
1358	1.85	152	197
1378	1.99	117	149
1305	10.62	117	125
1236	11.24	207	276
1299	10.25	122	137
1344	10.27	85	80
1290	11.88	118	138

mechanism, which they address with on-the-fly removal of small time scales. This removal was based on the quasi-steady-state and partial equilibrium approximations. Using these methods, they were able to develop a 52 species reduced mechanism whose shortest time scales were close to 10 ns. For comparison, their findings include results from the detailed mechanism which have been reproduced in Figures 3 and 4. These plots agree very closely to those found in the paper. Figure 3 is also an example of the NTC behavior of n-heptane combustion. For the higher temperatures, only one explosion can be observed as the reaction takes place. However, as the temperature decreases, two explosions take place. Further decreasing the temperature shortens the time between the explosions until again only one explosion occurs.

6.4 Individual Reaction Time Scale Analysis

After comparing the reaction mechanism with experimental results, the three sets of initial conditions in Figure 3 were used to perform a detailed analysis of the mechanism's time scales. First, each of the 2,738 reversible reactions were analyzed individually to compute their initial and final time scales. This was done as a starting point in determining the reactions causing the extremely small time scales in the reaction mechanism. The process was accomplished using a subroutine written to change the CHEMKIN input file before each calculation. Table 3 shows the equilibrium pressures and temperatures for the three initial temperatures used for the entire mechanism in Figure 3. These equilibrium conditions were used as the initial conditions for the the individual reaction calculations. As in Figure 3, all reactions were run under adiabatic, isochoric conditions.
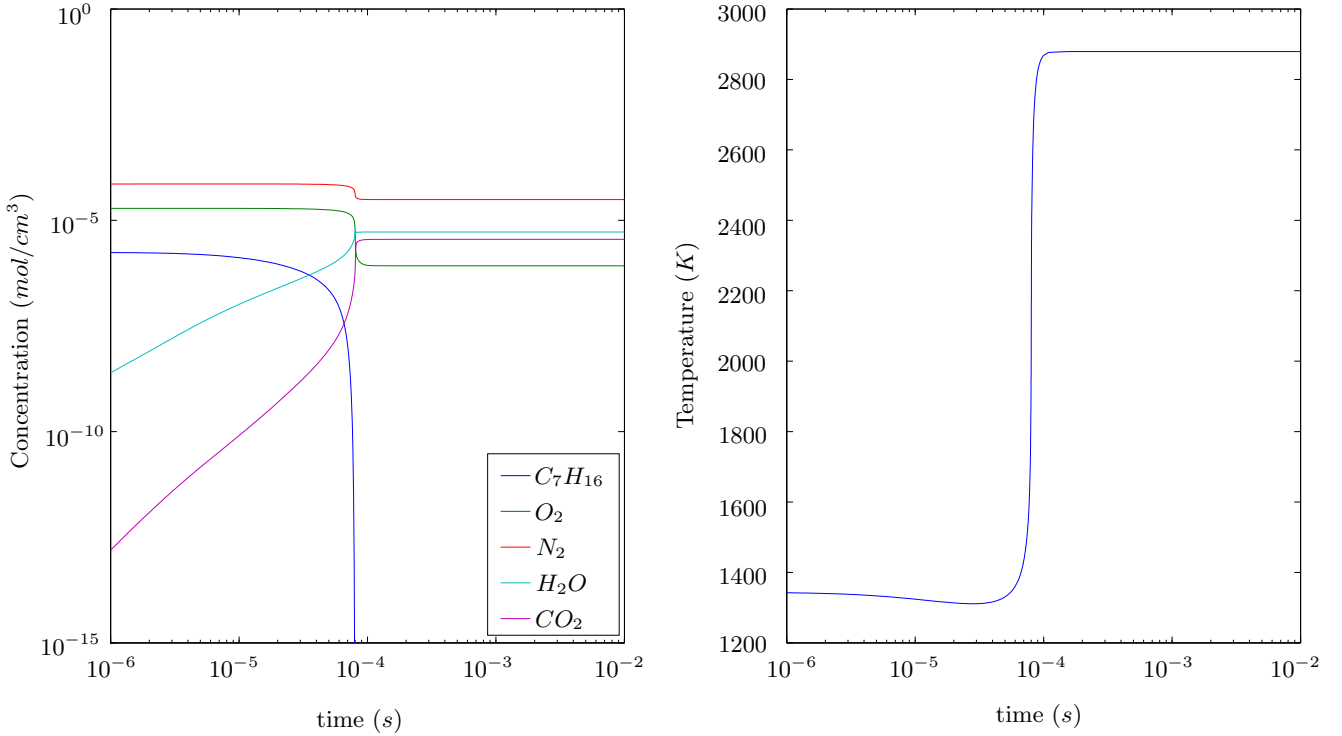
Figure 2: Temperature and concentration versus time plot for $T_i = 1344\ K$, $P = 10.27\ atm$, and $\phi = 1$.

All initial species amounts were set to $1 \times 10^{-5}\ mol$.

Table 3: Equilibrium temperatures and pressures for Figure 3

Initial Temperature (K)	Equilibrium Temperature (K)	Equilibrium Pressure $(dyne/cm^2)$
850	2274.1	8.368×10^8
1175	2534.7	6.757×10^8
1500	2779.3	5.822×10^8

To determine which reactions were not physical, the reaction time scales were compared to the molecular collision times. The reactions found to have non-physical time scales for one or more of the three sets of initial conditions can be found under Appendix A in Table 9. For the first set of initial conditions, $T_i = 2274.1\ K$ and $P_i = 8.368 \times 10^8\ dyne/cm^2$, 27 reactions were identified whose initial and/or final time scales were less than the predicted molecular collision times. The
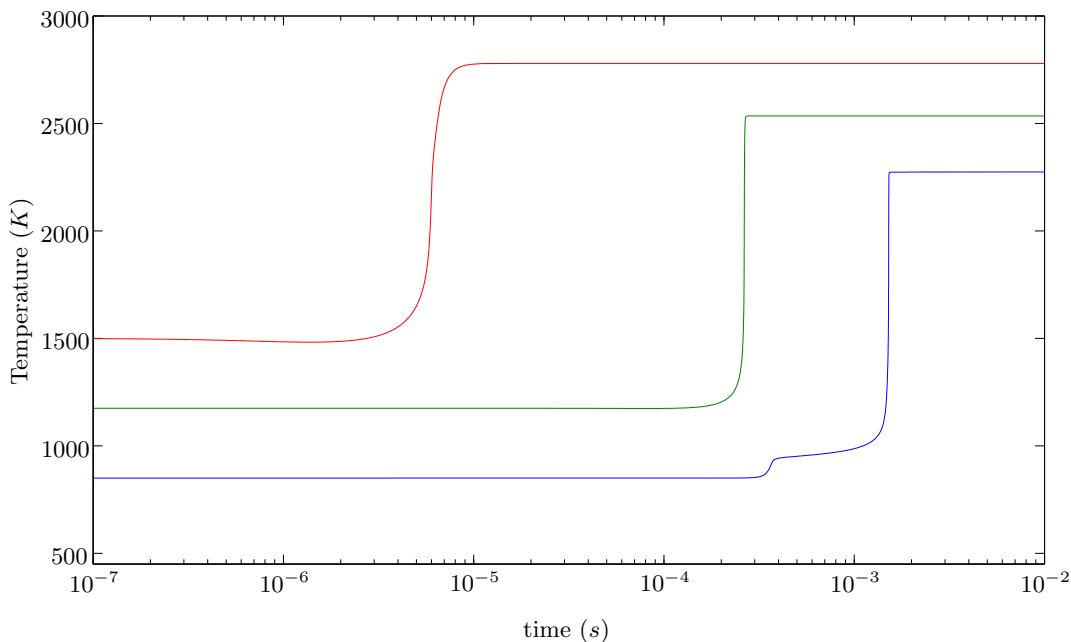
Figure 3: Temperature versus time plots for $T_i = 850\ K$, $1175\ K$, $1500\ K$ at $P_i = 30\ atm$, and ϕ=0.5 under adiabatic, isochoric conditions.

reactions (numbered corresponding to Table 9) and their time scales are listed in Table 6 sorted from fastest to slowest by initial time scale. For the second set of initial conditions, $T_i = 2534.7\ K$ and $P_i = 6.757 \times 10^8\ dyne/cm^2$, 118 reactions were found to be non-physical. They are listed in Table 7 along with their time scales. The last set of initial conditions, $T_i = 2779.3\ K$ and $P_i = 5.822 \times 10^8\ dyne/cm^2$, revealed 137 problem reactions. They can be found in Table 8.

6.5   Independent Time Scale Calculation

As a check on the results of the time scale calculations described in Section 6.4, the time scales for the fastest reaction in Tables 6 and 7 were calculated independently for an isothermal, isochoric case as in Section 5 at a temperature of $T = 1344\ K$. In the mechanism, the reaction is considered as a system of two irreversible reactions in Table 4. The forward and reverse reactions were also considered individually to determine which was the cause of the overall fast time scale. In the equations that follow, species $neoc5h9q2$-n will be indicated by a subscript $s1$ and species $neoc5ket$

23
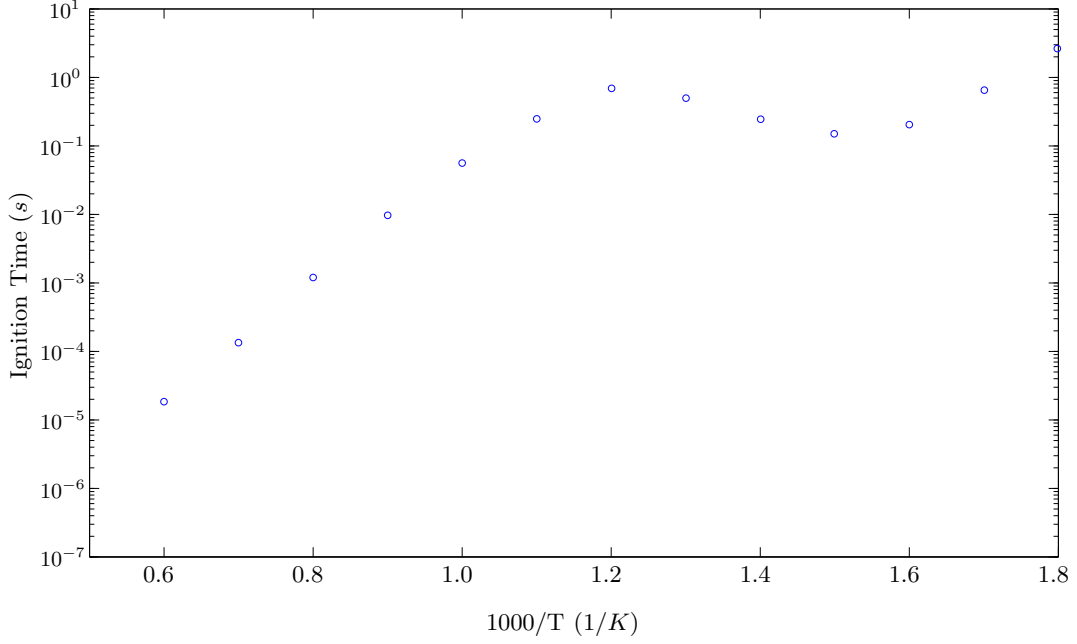
Figure 4: Ignition time for n-heptane at various temperatures at 1 atm and $\phi = 1$ under adiabatic, isobaric conditions.

Table 4: Reaction 1851 from Table 9

j	Reaction	a_j $[cm^3/(mol\ s\ K_j^\beta)]$	β_j	$\overline{E}_j$ $[cal/mol]$
1	$neoc5h9q2\text{-}n \rightarrow neoc5ket + oh$	9.00×10^{14}	0.00	1.500×10^3
2	$neoc5ket + oh \rightarrow neoc5h9q2\text{-}n$	1.668×10^9	1.58	3.188×10^4

with a subscript $s2$. The differential equations for the species concentrations are

$$\frac{d\overline{\rho}_{s1}}{dt} = -k_1\overline{\rho}_{s1} + k2\overline{\rho}_{s2}\overline{\rho}_{OH}, \tag{70}$$

$$\frac{d\overline{\rho}_{s2}}{dt} = k_1\overline{\rho}_{s1} - k2\overline{\rho}_{s2}\overline{\rho}_{OH}, \tag{71}$$

$$\frac{d\overline{\rho}_{OH}}{dt} = k_1\overline{\rho}_{s1} - k2\overline{\rho}_{s2}\overline{\rho}_{OH}, \tag{72}$$

with reaction rates defined as

$$r_1 = k_1\overline{\rho}_{s1}, \tag{73}$$

$$r_2 = k2\overline{\rho}_{s2}\overline{\rho}_{OH}. \tag{74}$$

24

The system can be written as

$$\frac{d}{dt}\begin{pmatrix}\overline{\rho}_{s1}\\\overline{\rho}_{s2}\\\overline{\rho}_{OH}\end{pmatrix}=\begin{pmatrix}-1 & 1\\1 & -1\\1 & -1\end{pmatrix}\begin{pmatrix}r_1\\r_2\end{pmatrix}. \tag{75}$$

Row reduction gives the form:

$$\frac{d}{dt}\begin{pmatrix}\overline{\rho}_{s2}\\\overline{\rho}_{s2}+\overline{\rho}_{s1}\\\overline{\rho}_{OH}-\overline{\rho}_{s2}\end{pmatrix}=\begin{pmatrix}1 & -1\\0 & 0\\0 & 0\end{pmatrix}\begin{pmatrix}r_1\\r_2\end{pmatrix}. \tag{76}$$

The following constraint equations are found by integrating the last two rows in Equation (76):

$$\overline{\rho}_{s2}+\overline{\rho}_{s1}=C_1, \tag{77}$$

$$\overline{\rho}_{OH}-\overline{\rho}_{s2}=C_2. \tag{78}$$

Using the initial concentrations $\hat{\overline{\rho}}_{s1}=\hat{\overline{\rho}}_{s2}=\hat{\overline{\rho}}_{OH}=1.66\times10^{-7}\ mol/cm^3$ we solve for the constants and find

$$\overline{\rho}_{s1} = 3.32\times10^{-7}-\overline{\rho}_{s2}, \tag{79}$$

$$\overline{\rho}_{OH} = \overline{\rho}_{s2}. \tag{80}$$

By substitution of Equations (79) and (80), Equation (71) can be written in terms of $\overline{\rho}_{s2}$ alone, leaving the differential equation

$$\frac{d\overline{\rho}_{s2}}{dt}=k_1(3.22\times10^{-7}-\overline{\rho}_{s2})-k_2\overline{\rho}_{s2}^2. \tag{81}$$

The plot of the solution to this reaction is shown in Figure 5. To calculate the time scales of the reaction Equation (81) is linearized using a Taylor series as in Section 5.2. At the initial state the
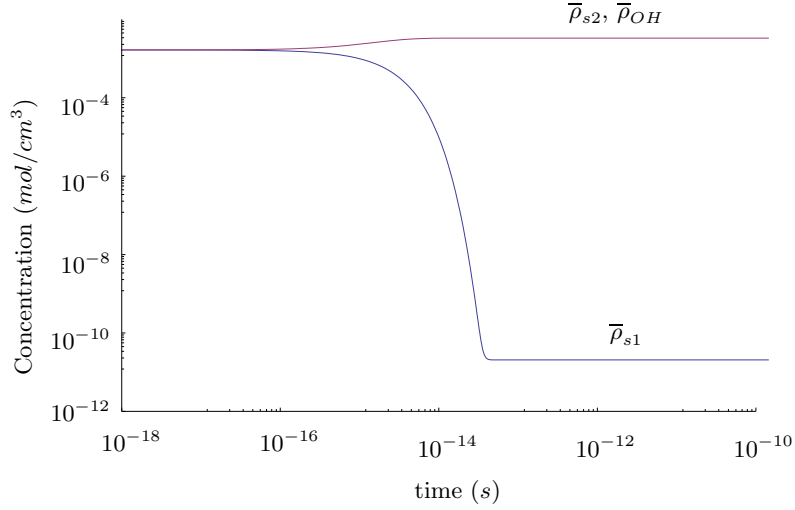
Figure 5: Species concentration versus time for reaction 1851.

Taylor series expansion of Equation (81) is

$$\frac{d}{dt}(\overline{\rho}_{s2} - \hat{\overline{\rho}}_{s2}) = k_1(3.22 \times 10^{-7} - \hat{\overline{\rho}}_{s2}) - k_2\hat{\overline{\rho}}_{s2}^2 - (k_1 + 2k_2\hat{\overline{\rho}}_{s2})(\overline{\rho}_{s2} - \hat{\overline{\rho}}_{s2}) + \ldots \tag{82}$$

The solution for $\overline{\rho}_{s2}$ is of the form

$$\overline{\rho}_{s2} = Ae^{-(k_1 + 2k_2\hat{\overline{\rho}}_{s2})t} + C. \tag{83}$$

Therefore, the initial time scale for the reaction is

$$\tau = \frac{1}{|-k_1 - 2k_2\hat{\overline{\rho}}_{s2}|} = 1.94837 \times 10^{-15} \ s. \tag{84}$$

In this equation $k_1 = 5.132 \times 10^{14} \ s^{-1}$ and $k_2 = 9.570 \times 10^8 \ s^{-1}$. The quantity $2k_2\overline{\rho}_{s2} = 3.191 \times 10^2$ $mol/(s \ cm^3)$. This means k_1 is the dominant term in the denominator, therefore, the small time scale is not effected by changing the initial conditions. Figure 5 shows the species concentrations begin substantial change in the neighborhood of τ. This time scale is much faster than the estimated time it would take for a molecular collision to occur; therefore, the reaction dynamics are not physical. The reaction has already reached equilibrium by 10^{-12} s, which is the order of magnitude for collisions. To further investigate the cause of the problem, time scales for the forward and reverse reactions were computed to be $\tau = 1.95 \times 10^{-15}$ s and $\tau = 1.57 \times 10^{-10}$ s, respectively.

26

This indicates the Arrhenius coefficients for the forward reaction are the cause of the non-physical reaction dynamics.

6.6 Reduced Mechanism Time Scale Analysis

After identifying the non-physical reactions for each of the three cases, the entire mechanism was run at initial temperatures of $T=850$ K, $T=1175$ K and $T=1500$ K, all at a initial pressure of 30 atm and $\phi=0.5$ for adiabatic, isochoric conditions as in [8]. Then, for each case reactions were removed one by one from the mechanism using another CHEMKIN input file changing subroutine. Reactions were removed fastest to slowest according to the time scales found during the corresponding individual reaction analysis. Each time the mechanism was reduced, the initial and equilibrium time scales were calculated and compared to the molecular collision times. Reactions were removed until the reduced system had physical initial and equilibrium time scales. Obtaining physical time scales for the reduced mechanism required the removal of many more reactions than were identified in Section 6.4. The results showed the removal of most reactions did not effect the initial and final time scales. For the most part, the time scales did not decrease gradually as reactions were taken away. Rather they remained constant until one the removal of one reaction would cause a change. The exception to this was near the beginning when the very fast reactions were taken out. In each case the initial time scale became physical before those at equilibrium.

The time scales for the full mechanisms at each initial temperature are shown in Table 5. At each temperature there was a drastic time scale improvement for the reduced mechanism over the full mechanism. Table 5 also shows the number of reactions found from the analysis in Section 6.4 that had to be removed in order for the initial and final time scales to be greater than the fastest molecular collision times. The reduced mechanisms were then compared to the full mechanism at each temperature. Figure 6 shows the temperature profiles for each reaction mechanism. The temperature profiles for the reduced mechanisms are in good agreement with those of the full mechanism. Surprisingly, closer agreement relative to the full mechanism is achieved for $T_i = 1500$ K than $T_i = 850$ K even though far more reactions were removed. One of the most important results to note from this reduction is the preservation of NTC behavior as seen for $T_i = 850$ K.

Table 5: Time scales for full and reduced mechanisms

T_i (K)	Full Mechanism		Reduced Mechanism		
	τ_i s	τ_{eq} (s)	τ_i (s)	τ_{eq} (s)	Reactions Removed
850	2.7006×10^{-15}	1.5486×10^{-15}	7.9169×10^{-12}	7.8978×10^{-13}	68
1175	2.1124×10^{-15}	1.4966×10^{-15}	3.3257×10^{-12}	1.2084×10^{-12}	140
1500	1.8379×10^{-15}	8.2029×10^{-16}	2.1802×10^{-12}	1.2572×10^{-12}	194
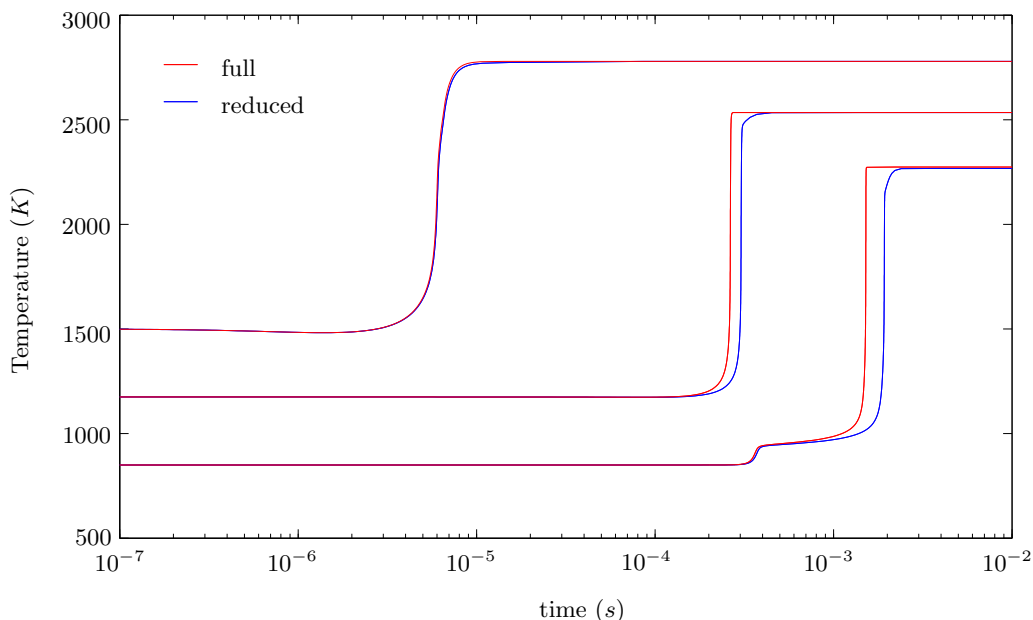
Figure 6: Temperature vs. time for reduced and full mechanisms.

7   Conclusions

Curran et al. [1] do not take time scales into account in their assessment of the mechanism. The mechanism was developed largely from a chemistry perspective without considering the mathematical implications of reaction rates. It is clear the fastest time scales for the n-heptane mechanism are non-physical and need to be addressed in order to improve the model. The approach taken here was to investigate the source of the problem by analyzing each reaction individually. The results of this analysis show there are several reactions that consistently have non-physical dynamics across several different conditions. Reactions found to have time scales less than molecular collision times from the individual analysis were assumed to contribute to the fast time scales for the full mech-

anism. To increase the full mechanism time scales to physical values without taking away certain reaction characteristics such as NTC behavior and ignition delay, problem reactions were removed one by one. This approach helped to ensure reactions were not taken away unnecessarily. It was not determined how one of these reduced systems behaves for other conditions or whether this was an acceptable approach to find a general reduced system. In a sense, each of the reduced mechanisms considered here was tailor made for a specific set of conditions. To make a reduced system for a certain set of initial conditions, the full reaction mechanism was first run at those conditions to determine the equilibrium conditions to used as initial conditions for the individual reaction analysis. Therefore, each reduced system was developed by removing a sorted list of reactions specifically for the intended initial conditions for the system. However, comparisons between the reduced mechanisms found by this process and the complete mechanisms were in good agreement and the time scale issues were corrected. This indicates the method used here to remove the non-physical time scales was effective.

References

[1] H. J. Curran, P. Gaffuri, W. J. Pitz, and C. K. Westbrook. A comprehensive modeling study of n-heptane. *Combustion and Flame*, 114(1):149–177, 1998.

[2] F. Zhao, T. W. Asmus, D. N. Assanis, J. E. Dec, J. A. Eng, and P. M. Najt, eds. *Homogeneous Charge Compression Ignition (HCCI) Engines*. Society of Automotive Engineers, Warrendale, PA, 2003.

[3] B. M. Gauthier, D. F. Davidson, and R. K. Hanson. Shock tube determination of ignition delay times in full-blend and surrogate fuel mixtures. *Combustion and Flame*, 139(4):300–311, 2004.

[4] W. G. Vincenti and C. H. Kruger Jr. *Introduction to Physical Gas Dynamics*. John Wiley and Sons, Inc., New York, 1967.

[5] S. Singh. "Rational reduction of reactive flow models and efficient computation of their solution". PhD thesis, University of Notre Dame, Notre Dame, IN, March 2003.

[6] R. J. Kee, F. M. Rupley, E. Meeks, and J. A. Miller. Chemkin-III: A Fortran Chemical Kinetics Package for the Analysis of Gas Phase Chemical and Plasma Kinetics. Technical Report SAND96-8216, Sandia National Laboratories, Livermore, CA, 1996.

[7] A. N. Al-Khateeb, J. M. Powers, S. Paolucci, A. J. Sommese, J. A. Diller, J. D. Hauenstein, and J. D. Mengers. One-dimensional slow invariant manifolds for spatially homogeneous reactive systems. *Journal of Chemical Physics*, 131(2):024118, 2009.

[8] T. Lu, C. K. Law, C. S. Yoo, and J. H. Chen. Dynamic stiffness removal for direct numerical simulations. *Combustion and Flame*, 156(8):1542–1551, 2009.

[9] A. C. Hindmarsh. ODEPACK, a systematized collection of ODE solvers. In R. S. Stepleman et al., editor, *Scientific Computing*, pages 55–64, North-Holland, Amsterdam, 1983.

[10] Visual Numerics Inc. *IMSL Fortran Library User's Guide*. International Mathematical and Statistical Libraries, San Ramon, CA, 2003.

[11] W. H. Press, B. P. Flannery, S. A. Teukolsky, and W. T. Vetterling. *Numerical Recipes: The Art of Scientific Computing (FORTRAN Version)*. Press Syndicate of the University of Cambridge, New York, 1989.

Appendix A: Individual Reaction Time Scales

These are the reactions found to have non-physical time scales from the analysis in Section 6.4. They are sorted fasted to slowest according to initial time scale.

Table 6: Reactions with non-physical time scales for $T_i = 2274.1\ K$ and $P_i = 8.368 \times 10^8\ dyne/cm^2$

Reaction	$\tau_i\ (s)$	$\tau_{eq}\ (s)$
1851	$1.5487556485352769 \times 10^{-15}$	$1.5483445540365251 \times 10^{-15}$
725	$6.2444931131328749 \times 10^{-15}$	$6.2790336304157846 \times 10^{-15}$
726	$9.7030531362904746 \times 10^{-15}$	$9.7602533627293191 \times 10^{-15}$
1705	$1.1633240434118526 \times 10^{-14}$	$1.1635295665228966 \times 10^{-14}$
1647	$1.8858988253441932 \times 10^{-14}$	$1.8907319679699537 \times 10^{-14}$
727	$2.5311575198363325 \times 10^{-14}$	$2.5250672891238786 \times 10^{-14}$
728	$2.5317378023270418 \times 10^{-14}$	$2.5244893702047646 \times 10^{-14}$
1398	$2.6097178459297332 \times 10^{-14}$	$2.6038657039725654 \times 10^{-14}$
1487	$4.3025327193714666 \times 10^{-14}$	$4.3040184893889784 \times 10^{-14}$
718	$8.4378250739293108 \times 10^{-14}$	$8.4406984295019587 \times 10^{-14}$
719	$8.4415236354005607 \times 10^{-14}$	$8.4369993726411803 \times 10^{-14}$
1138	$1.0235718342673776 \times 10^{-13}$	$1.0263500956763352 \times 10^{-13}$
1849	$1.5742241957978209 \times 10^{-13}$	$1.5673332664470601 \times 10^{-13}$
777	$1.9793190349021273 \times 10^{-13}$	$1.9847041307263636 \times 10^{-13}$
1633	$2.1501889806597534 \times 10^{-13}$	$2.1494476179575313 \times 10^{-13}$
1461	$2.1504079406491892 \times 10^{-13}$	$2.1492288740384553 \times 10^{-13}$
1392	$2.1647328059551167 \times 10^{-13}$	$2.1707656293801643 \times 10^{-13}$
1399	$2.2148945750798683 \times 10^{-13}$	$2.2115226229708487 \times 10^{-13}$
830	$2.4041872964302122 \times 10^{-13}$	$2.4037319712868599 \times 10^{-13}$
1869	$2.7043845709260328 \times 10^{-13}$	$2.7043331820482370 \times 10^{-13}$
1110	$2.8480623518826533 \times 10^{-13}$	$2.8470028768847806 \times 10^{-13}$
1490	$2.9110552984558256 \times 10^{-13}$	$2.9148905186515330 \times 10^{-13}$
1320	$3.5492284400507401 \times 10^{-13}$	$3.5484484468188864 \times 10^{-13}$
1847	$3.6098525534390635 \times 10^{-13}$	$3.6098178779425059 \times 10^{-13}$
1145	$3.6262855238122125 \times 10^{-13}$	$3.6373508707016997 \times 10^{-13}$
1148	$3.9806534865882597 \times 10^{-13}$	$3.9926202389378549 \times 10^{-13}$
831	$4.1391449229463362 \times 10^{-13}$	$4.1382553480334145 \times 10^{-13}$

Table 7: Reactions with non-physical time scales for $T_i = 2534.7\ K$ and $P_i = 6.757 \times 10^8\ dyne/cm^2$

Reaction	$\tau_i\ (s)$	$\tau_{eq}\ (s)$
1851	$1.4967445044461254 \times 10^{-15}$	$1.4964221447951531 \times 10^{-15}$
725	$2.0872230560340603 \times 10^{-15}$	$2.0960434141929594 \times 10^{-15}$
726	$3.0337400213444421 \times 10^{-15}$	$3.0473907260894428 \times 10^{-15}$

Table 7 – continued from previous page

Reaction	τ_i (s)	τ_{eq} (s)
1705	$6.8508579738540876 \times 10^{-15}$	$6.8508556508613072 \times 10^{-15}$
1647	$1.1177499869575820 \times 10^{-14}$	$1.1199274480750594 \times 10^{-14}$
727	$1.4327664578449061 \times 10^{-14}$	$1.4297875231158972 \times 10^{-14}$
728	$1.4330260958483956 \times 10^{-14}$	$1.4295287685960405 \times 10^{-14}$
1398	$1.8970807717936387 \times 10^{-14}$	$1.8936983975101738 \times 10^{-14}$
1487	$4.5046245428431124 \times 10^{-14}$	$4.5064865349762897 \times 10^{-14}$
718	$5.4763133986219064 \times 10^{-14}$	$5.4773472611752014 \times 10^{-14}$
719	$5.4782070869137769 \times 10^{-14}$	$5.4754535107791842 \times 10^{-14}$
1138	$5.9049751094012413 \times 10^{-14}$	$5.9162049438929607 \times 10^{-14}$
1849	$7.4801815957567088 \times 10^{-14}$	$7.4522111114344058 \times 10^{-14}$
777	$1.1406308226518556 \times 10^{-13}$	$1.1428074090274809 \times 10^{-13}$
1392	$1.2123862283362001 \times 10^{-13}$	$1.2148266980019722 \times 10^{-13}$
1399	$1.6087018648823621 \times 10^{-13}$	$1.6067549259595051 \times 10^{-13}$
830	$1.6144508933082101 \times 10^{-13}$	$1.6140905617786716 \times 10^{-13}$
1633	$1.7242741234362589 \times 10^{-13}$	$1.7237285616405684 \times 10^{-13}$
1461	$1.7244129312201551 \times 10^{-13}$	$1.7235898625880461 \times 10^{-13}$
1490	$1.7850058905103854 \times 10^{-13}$	$1.7868000873009864 \times 10^{-13}$
1869	$1.9267186246292159 \times 10^{-13}$	$1.9266429621329388 \times 10^{-13}$
1145	$2.0143733955806278 \times 10^{-13}$	$2.0188465850473487 \times 10^{-13}$
1148	$2.2227378375250155 \times 10^{-13}$	$2.2275916048185156 \times 10^{-13}$
1110	$2.2361201555311028 \times 10^{-13}$	$2.2353945892326048 \times 10^{-13}$
1055	$2.7258672044057897 \times 10^{-13}$	$2.7321235875595775 \times 10^{-13}$
1433	$2.7820236175757005 \times 10^{-13}$	$2.7963096862134829 \times 10^{-13}$
1420	$2.7823705300367347 \times 10^{-13}$	$2.7966334346183790 \times 10^{-13}$
1426	$2.7824039334099182 \times 10^{-13}$	$2.7965997721133142 \times 10^{-13}$
2087	$2.7824091220374001 \times 10^{-13}$	$2.7965945580458245 \times 10^{-13}$
1416	$2.7824292511125455 \times 10^{-13}$	$2.7965743159309397 \times 10^{-13}$
1407	$2.7824316308133090 \times 10^{-13}$	$2.7965718803150308 \times 10^{-13}$
2092	$2.7824855347185133 \times 10^{-13}$	$2.7965176213320886 \times 10^{-13}$
2396	$2.7824866702795523 \times 10^{-13}$	$2.7965164794913617 \times 10^{-13}$
2397	$2.7824866702795523 \times 10^{-13}$	$2.7965164794913617 \times 10^{-13}$
1430	$2.7827867864619154 \times 10^{-13}$	$2.7962137818304900 \times 10^{-13}$
1403	$2.7830174475078868 \times 10^{-13}$	$2.7959808946032423 \times 10^{-13}$
1410	$2.7830315079574559 \times 10^{-13}$	$2.7959667643703767 \times 10^{-13}$
1429	$2.7831236307643215 \times 10^{-13}$	$2.7958737016132531 \times 10^{-13}$
1421	$2.7831361813468751 \times 10^{-13}$	$2.7958610597576472 \times 10^{-13}$
1408	$2.7832409360140451 \times 10^{-13}$	$2.7957557246054758 \times 10^{-13}$
1417	$2.7832460891093893 \times 10^{-13}$	$2.7957505486483170 \times 10^{-13}$
2083	$2.7832504578281725 \times 10^{-13}$	$2.7957461662038825 \times 10^{-13}$
2088	$2.7832518161869757 \times 10^{-13}$	$2.7957443821443495 \times 10^{-13}$
2391	$2.7833601052737498 \times 10^{-13}$	$2.7956354965826331 \times 10^{-13}$
1427	$2.7837496983377630 \times 10^{-13}$	$2.7952429737999158 \times 10^{-13}$
1419	$2.7837604080955476 \times 10^{-13}$	$2.7952322451068170 \times 10^{-13}$
1423	$2.7837839422374264 \times 10^{-13}$	$2.7952085129406878 \times 10^{-13}$

33

Table 7 – continued from previous page

Reaction	τ_i (s)	τ_{eq} (s)
1404	$2.7838819174404614 \times 10^{-13}$	$2.7951098154665281 \times 10^{-13}$
2386	$2.7840175273236363 \times 10^{-13}$	$2.7949731889747556 \times 10^{-13}$
1411	$2.7845339202870738 \times 10^{-13}$	$2.7944534838962172 \times 10^{-13}$
1418	$2.7849040827192626 \times 10^{-13}$	$2.7940811011040978 \times 10^{-13}$
1320	$2.9697469924103356 \times 10^{-13}$	$2.9692038274660453 \times 10^{-13}$
831	$3.0066280172798123 \times 10^{-13}$	$3.0059327518295142 \times 10^{-13}$
837	$3.0722700170516570 \times 10^{-13}$	$3.0882712985373200 \times 10^{-13}$
609	$3.0723017917817459 \times 10^{-13}$	$3.0882363785242308 \times 10^{-13}$
834	$3.0723302494690339 \times 10^{-13}$	$3.0882243751894807 \times 10^{-13}$
1105	$3.0723305635127245 \times 10^{-13}$	$3.0882275247345863 \times 10^{-13}$
1108	$3.0723305635127245 \times 10^{-13}$	$3.0882274840039314 \times 10^{-13}$
2022	$3.0723310629191651 \times 10^{-13}$	$3.0882195085492850 \times 10^{-13}$
2309	$3.0723382967317092 \times 10^{-13}$	$3.0882238730835483 \times 10^{-13}$
1319	$3.0723469758143365 \times 10^{-13}$	$3.0881823939381636 \times 10^{-13}$
1243	$3.0724503121842703 \times 10^{-13}$	$3.0880673107346435 \times 10^{-13}$
2310	$3.0836652246676870 \times 10^{-13}$	$3.0991839562916166 \times 10^{-13}$
2312	$3.0836652246676888 \times 10^{-13}$	$3.0991839562916534 \times 10^{-13}$
2311	$3.0837625936226787 \times 10^{-13}$	$3.0993814659246781 \times 10^{-13}$
2024	$3.0837648335617205 \times 10^{-13}$	$3.0994994068824218 \times 10^{-13}$
2023	$3.0837648335617263 \times 10^{-13}$	$3.0994994068824226 \times 10^{-13}$
606	$3.5705867881710720 \times 10^{-13}$	$3.5730328822617445 \times 10^{-13}$
1847	$3.6211300153013837 \times 10^{-13}$	$3.6211884976764415 \times 10^{-13}$
2079	$3.6702495153301742 \times 10^{-13}$	$3.6912700222383386 \times 10^{-13}$
2086	$3.6723997208840800 \times 10^{-13}$	$3.6891039450009870 \times 10^{-13}$
2389	$3.6724058253314129 \times 10^{-13}$	$3.6890979424760673 \times 10^{-13}$
2390	$3.6724512573787638 \times 10^{-13}$	$3.6890520994328382 \times 10^{-13}$
2082	$3.6724678183246939 \times 10^{-13}$	$3.6890354079603505 \times 10^{-13}$
2385	$3.6724699295669030 \times 10^{-13}$	$3.6890334196669960 \times 10^{-13}$
1415	$3.6724717751127303 \times 10^{-13}$	$3.6890314709567349 \times 10^{-13}$
2081	$3.6724768307226068 \times 10^{-13}$	$3.6890264343943269 \times 10^{-13}$
2384	$3.6725046748245136 \times 10^{-13}$	$3.6889984748337796 \times 10^{-13}$
2395	$3.6726370424805701 \times 10^{-13}$	$3.6888650056844163 \times 10^{-13}$
1406	$3.6732383628374672 \times 10^{-13}$	$3.6882588029037100 \times 10^{-13}$
1414	$3.6732480016772033 \times 10^{-13}$	$3.6882492315751527 \times 10^{-13}$
2085	$3.6732717883157600 \times 10^{-13}$	$3.6882253005898811 \times 10^{-13}$
2080	$3.6732787986134579 \times 10^{-13}$	$3.6882182781056594 \times 10^{-13}$
2388	$3.6733036339158422 \times 10^{-13}$	$3.6881933055903540 \times 10^{-13}$
2383	$3.6733062168096238 \times 10^{-13}$	$3.6881907081257284 \times 10^{-13}$
1432	$3.6733646198389565 \times 10^{-13}$	$3.6881316906084605 \times 10^{-13}$
2091	$3.6733892179369598 \times 10^{-13}$	$3.6881066987125455 \times 10^{-13}$
2399	$3.6734896301437225 \times 10^{-13}$	$3.6880060118416735 \times 10^{-13}$
2394	$3.6734956743702725 \times 10^{-13}$	$3.6879996392084591 \times 10^{-13}$
1402	$3.6735298836895991 \times 10^{-13}$	$3.6879651750288547 \times 10^{-13}$
2398	$3.6735398920261613 \times 10^{-13}$	$3.6879547967524031 \times 10^{-13}$

Table 7 – continued from previous page

Reaction	$\tau_i \ (s)$	$\tau_{eq} \ (s)$
1405	$3.6735518097746138 \times 10^{-13}$	$3.6879432363626701 \times 10^{-13}$
1413	$3.6736030924581309 \times 10^{-13}$	$3.6878916710140608 \times 10^{-13}$
1422	$3.6738854892623163 \times 10^{-13}$	$3.6876073438558894 \times 10^{-13}$
2089	$3.6738905775053721 \times 10^{-13}$	$3.6876022386478908 \times 10^{-13}$
2090	$3.6738944856489164 \times 10^{-13}$	$3.6875984129533936 \times 10^{-13}$
2382	$3.6740701752670510 \times 10^{-13}$	$3.6874211308775999 \times 10^{-13}$
1425	$3.6742654525159857 \times 10^{-13}$	$3.6872247543813441 \times 10^{-13}$
2392	$3.6743934635422359 \times 10^{-13}$	$3.6870958088072920 \times 10^{-13}$
2393	$3.6744250157204617 \times 10^{-13}$	$3.6870642073537399 \times 10^{-13}$
1409	$3.6747195158762960 \times 10^{-13}$	$3.6867679857623910 \times 10^{-13}$
2084	$3.6747999295053457 \times 10^{-13}$	$3.6866872386990268 \times 10^{-13}$
2387	$3.6753601875523816 \times 10^{-13}$	$3.6861236667362762 \times 10^{-13}$
1245	$4.0786354473230607 \times 10^{-13}$	$4.0987429814620970 \times 10^{-13}$
610	$4.0787227071174978 \times 10^{-13}$	$4.0997150347682689 \times 10^{-13}$
1107	$4.0787566565772053 \times 10^{-13}$	$4.0996354855536126 \times 10^{-13}$
835	$4.0787622900454608 \times 10^{-13}$	$4.0997134055501459 \times 10^{-13}$
1244	$4.0789770673880188 \times 10^{-13}$	$4.0994361266482588 \times 10^{-13}$
607	$4.1481178115033677 \times 10^{-13}$	$4.1524820896587205 \times 10^{-13}$
1431	$4.8941787568319519 \times 10^{-13}$	$4.9117033612324139 \times 10^{-13}$
1412	$4.8948222722326147 \times 10^{-13}$	$4.9110558717663721 \times 10^{-13}$
1424	$4.8949704490152088 \times 10^{-13}$	$4.9109068858088252 \times 10^{-13}$
1428	$4.8964578480568042 \times 10^{-13}$	$4.9094114993602256 \times 10^{-13}$
1018	$5.0858905301744972 \times 10^{-13}$	$5.1123933995263311 \times 10^{-13}$
1111	$5.6013231804383157 \times 10^{-13}$	$5.5995953133411636 \times 10^{-13}$
1550	$5.6801644496389381 \times 10^{-13}$	$5.6803719957088017 \times 10^{-13}$
673	$5.8867118016629050 \times 10^{-13}$	$5.9038361430608788 \times 10^{-13}$
2535	$5.9823745530776904 \times 10^{-13}$	$5.9844659482755507 \times 10^{-13}$

Table 8: Reactions with non-physical time scales for $T_i = 2779.3 \ K$ and $P_i = 5.822 \times 10^8 \ dyne/cm^2$

Reaction	$\tau_i \ (s)$	$\tau_{eq} \ (s)$
725	$8.9861510467673167 \times 10^{-16}$	$9.0163327093863650 \times 10^{-16}$
726	$1.2444470659697626 \times 10^{-15}$	$1.2488949782189145 \times 10^{-15}$
1851	$1.4580044316256979 \times 10^{-15}$	$1.4577405169897499 \times 10^{-15}$
1705	$4.5471577123682323 \times 10^{-15}$	$4.5466287232079425 \times 10^{-15}$
1647	$7.4802977839219054 \times 10^{-15}$	$7.4918153730024040 \times 10^{-15}$
727	$9.2562513130229611 \times 10^{-15}$	$9.2391699368468387 \times 10^{-15}$
728	$9.2576230755200406 \times 10^{-15}$	$9.2378023720800524 \times 10^{-15}$
1398	$1.4849845047887335 \times 10^{-14}$	$1.4827981326878660 \times 10^{-14}$

Table 8 – continued from previous page

Reaction	$\tau_i \ (s)$	$\tau_{eq} \ (s)$
718	$3.9295688785773777 \times 10^{-14}$	$3.9299388064192557 \times 10^{-14}$
719	$3.9306865165224583 \times 10^{-14}$	$3.9288211707107514 \times 10^{-14}$
1138	$3.9825807782732724 \times 10^{-14}$	$3.9881099768564404 \times 10^{-14}$
1849	$4.2111834896015319 \times 10^{-14}$	$4.1973561040512024 \times 10^{-14}$
1487	$4.7253273065457204 \times 10^{-14}$	$4.7274811089723210 \times 10^{-14}$
777	$7.6858516637512988 \times 10^{-14}$	$7.6965676997606645 \times 10^{-14}$
1392	$7.9418936970493164 \times 10^{-14}$	$7.9539206217326690 \times 10^{-14}$
830	$1.1891757416250863 \times 10^{-13}$	$1.1888896684894741 \times 10^{-13}$
1490	$1.2261799145737096 \times 10^{-13}$	$1.2271536411512034 \times 10^{-13}$
1399	$1.2578431062068598 \times 10^{-13}$	$1.2565858974362409 \times 10^{-13}$
1145	$1.3103388916934966 \times 10^{-13}$	$1.3125433451973492 \times 10^{-13}$
1433	$1.3363640799474295 \times 10^{-13}$	$1.3419158220793257 \times 10^{-13}$
1420	$1.3365489201790526 \times 10^{-13}$	$1.3418638569965187 \times 10^{-13}$
1426	$1.3365636986369809 \times 10^{-13}$	$1.3418489909595708 \times 10^{-13}$
2087	$1.3365666446657278 \times 10^{-13}$	$1.3418460497933498 \times 10^{-13}$
1416	$1.3365759545457769 \times 10^{-13}$	$1.3418366671472959 \times 10^{-13}$
1407	$1.3365774321404633 \times 10^{-13}$	$1.3418351921236682 \times 10^{-13}$
2396	$1.3366024262108724 \times 10^{-13}$	$1.3418100556612416 \times 10^{-13}$
2397	$1.3366024262108724 \times 10^{-13}$	$1.3418100556612416 \times 10^{-13}$
2092	$1.3366024878906808 \times 10^{-13}$	$1.3418099906632819 \times 10^{-13}$
1430	$1.3367237940731598 \times 10^{-13}$	$1.3416878636643861 \times 10^{-13}$
1403	$1.3368036306687623 \times 10^{-13}$	$1.3416073821798793 \times 10^{-13}$
1410	$1.3368096542255572 \times 10^{-13}$	$1.3416013441946206 \times 10^{-13}$
1429	$1.3368368312718826 \times 10^{-13}$	$1.3415739197856151 \times 10^{-13}$
1421	$1.3368436290817303 \times 10^{-13}$	$1.3415671032220597 \times 10^{-13}$
2088	$1.3368810750506586 \times 10^{-13}$	$1.3415293671861914 \times 10^{-13}$
1408	$1.3368968541596393 \times 10^{-13}$	$1.3415136221885446 \times 10^{-13}$
1417	$1.3368990642749987 \times 10^{-13}$	$1.3415114041335165 \times 10^{-13}$
2083	$1.3369011045837220 \times 10^{-13}$	$1.3415093618593974 \times 10^{-13}$
2391	$1.3369368312281544 \times 10^{-13}$	$1.3414733652667754 \times 10^{-13}$
1427	$1.3370932823397383 \times 10^{-13}$	$1.3413159866220608 \times 10^{-13}$
1419	$1.3370992254933964 \times 10^{-13}$	$1.3413100185040592 \times 10^{-13}$
1423	$1.3371080578042680 \times 10^{-13}$	$1.3413011399262813 \times 10^{-13}$
1404	$1.3371473472101232 \times 10^{-13}$	$1.3412615973247117 \times 10^{-13}$
2386	$1.3371957098248457 \times 10^{-13}$	$1.3412129694849084 \times 10^{-13}$
1411	$1.3374102804684433 \times 10^{-13}$	$1.3409973223815796 \times 10^{-13}$
1418	$1.3375603052503715 \times 10^{-13}$	$1.3408465895851323 \times 10^{-13}$
1148	$1.4522954630057495 \times 10^{-13}$	$1.4546934393314348 \times 10^{-13}$
1633	$1.4554653192661489 \times 10^{-13}$	$1.4550380902293445 \times 10^{-13}$
1461	$1.4555615517359424 \times 10^{-13}$	$1.4549419276481386 \times 10^{-13}$
837	$1.4629596162376908 \times 10^{-13}$	$1.4691260221924454 \times 10^{-13}$
609	$1.4629710858198706 \times 10^{-13}$	$1.4691133283713000 \times 10^{-13}$
834	$1.4629818621085231 \times 10^{-13}$	$1.4691055827411759 \times 10^{-13}$
1105	$1.4629823632368608 \times 10^{-13}$	$1.4691058644651749 \times 10^{-13}$

Table 8 – continued from previous page

Reaction	τ_i (s)	τ_{eq} (s)
1108	$1.4629823632368608 \times 10^{-13}$	$1.4691058644647093 \times 10^{-13}$
2022	$1.4629827655729097 \times 10^{-13}$	$1.4691038635905795 \times 10^{-13}$
2309	$1.4629850458259104 \times 10^{-13}$	$1.4691039094405589 \times 10^{-13}$
1319	$1.4629921426485701 \times 10^{-13}$	$1.4690901541235403 \times 10^{-13}$
1243	$1.4630326607259407 \times 10^{-13}$	$1.4690471965487573 \times 10^{-13}$
1869	$1.4851378153273584 \times 10^{-13}$	$1.4850591323031739 \times 10^{-13}$
2310	$1.4916432649863482 \times 10^{-13}$	$1.4977166873015115 \times 10^{-13}$
2312	$1.4916432649863487 \times 10^{-13}$	$1.4977166873015109 \times 10^{-13}$
2024	$1.4916542653115310 \times 10^{-13}$	$1.4977895509359889 \times 10^{-13}$
2023	$1.4916542653115332 \times 10^{-13}$	$1.4977895509359898 \times 10^{-13}$
2311	$1.4916643469180628 \times 10^{-13}$	$1.4977593569002274 \times 10^{-13}$
1055	$1.7617247885050751 \times 10^{-13}$	$1.7647872886236988 \times 10^{-13}$
2079	$1.7753911381560288 \times 10^{-13}$	$1.7835704796374592 \times 10^{-13}$
2086	$1.7763676013258179 \times 10^{-13}$	$1.7825881134546295 \times 10^{-13}$
2389	$1.7763759811306405 \times 10^{-13}$	$1.7825797297068526 \times 10^{-13}$
2390	$1.7763914442246604 \times 10^{-13}$	$1.7825641516530633 \times 10^{-13}$
2082	$1.7763995111251052 \times 10^{-13}$	$1.7825560321611920 \times 10^{-13}$
1415	$1.7764017779945429 \times 10^{-13}$	$1.7825537690257036 \times 10^{-13}$
2385	$1.7764061432299227 \times 10^{-13}$	$1.7825494095967249 \times 10^{-13}$
2081	$1.7764096861351975 \times 10^{-13}$	$1.7825458486282115 \times 10^{-13}$
2384	$1.7764231992789883 \times 10^{-13}$	$1.7825322774609631 \times 10^{-13}$
2395	$1.7764734549303398 \times 10^{-13}$	$1.7824816904979334 \times 10^{-13}$
1406	$1.7766999277452094 \times 10^{-13}$	$1.7822537587095661 \times 10^{-13}$
1414	$1.7767098101543435 \times 10^{-13}$	$1.7822438658223049 \times 10^{-13}$
2085	$1.7767200364640603 \times 10^{-13}$	$1.7822335947796297 \times 10^{-13}$
2080	$1.7767246025426164 \times 10^{-13}$	$1.7822290140640713 \times 10^{-13}$
2388	$1.7767353005556639 \times 10^{-13}$	$1.7822182691090456 \times 10^{-13}$
2383	$1.7767370287550211 \times 10^{-13}$	$1.7822165344429739 \times 10^{-13}$
2091	$1.7767507518438324 \times 10^{-13}$	$1.7822026004700202 \times 10^{-13}$
1432	$1.7767526079126683 \times 10^{-13}$	$1.7822007915826856 \times 10^{-13}$
2398	$1.7767998665215059 \times 10^{-13}$	$1.7821531396143784 \times 10^{-13}$
2394	$1.7768000178317632 \times 10^{-13}$	$1.7821531041640705 \times 10^{-13}$
2399	$1.7768118244388786 \times 10^{-13}$	$1.7821413212234627 \times 10^{-13}$
1402	$1.7768154967943506 \times 10^{-13}$	$1.7821375268776256 \times 10^{-13}$
1405	$1.7768307184615296 \times 10^{-13}$	$1.7821222713836002 \times 10^{-13}$
1413	$1.7768541800690110 \times 10^{-13}$	$1.7820987014204976 \times 10^{-13}$
1422	$1.7769670126148077 \times 10^{-13}$	$1.7819852808259831 \times 10^{-13}$
2089	$1.7769691443787636 \times 10^{-13}$	$1.7819831421356676 \times 10^{-13}$
2090	$1.7769766721937836 \times 10^{-13}$	$1.7819756115214522 \times 10^{-13}$
2382	$1.7770216906175968 \times 10^{-13}$	$1.7819302168553619 \times 10^{-13}$
1425	$1.7771106775269065 \times 10^{-13}$	$1.7818408364132265 \times 10^{-13}$
2392	$1.7771525293898829 \times 10^{-13}$	$1.7817987389762617 \times 10^{-13}$
2393	$1.7771732598014978 \times 10^{-13}$	$1.7817779562049784 \times 10^{-13}$
1409	$1.7772953419641158 \times 10^{-13}$	$1.7816553166871145 \times 10^{-13}$

Table 8 – continued from previous page

Reaction	$\tau_i\ (s)$	$\tau_{eq}\ (s)$
2084	$1.7773369755372215 \times 10^{-13}$	$1.7816135426815951 \times 10^{-13}$
2387	$1.7775492238788326 \times 10^{-13}$	$1.7814003266681723 \times 10^{-13}$
1110	$1.8761764257380856 \times 10^{-13}$	$1.8756417033053172 \times 10^{-13}$
610	$1.9729807809767008 \times 10^{-13}$	$1.9812147696733394 \times 10^{-13}$
835	$1.9729954895206374 \times 10^{-13}$	$1.9812075569532794 \times 10^{-13}$
1107	$1.9729978755363767 \times 10^{-13}$	$1.9811877476070299 \times 10^{-13}$
1245	$1.9730190644092742 \times 10^{-13}$	$1.9809623095159212 \times 10^{-13}$
1244	$1.9730877404330611 \times 10^{-13}$	$1.9811012762860722 \times 10^{-13}$
1431	$2.3286004114376881 \times 10^{-13}$	$2.3348854379086732 \times 10^{-13}$
1412	$2.3288550631712961 \times 10^{-13}$	$2.3346295698087127 \times 10^{-13}$
1424	$2.3289152981002612 \times 10^{-13}$	$2.3345690628718687 \times 10^{-13}$
1428	$2.3295042368513013 \times 10^{-13}$	$2.3339777095282583 \times 10^{-13}$
831	$2.3574729841016344 \times 10^{-13}$	$2.3569151328715243 \times 10^{-13}$
1018	$2.4014919445663478 \times 10^{-13}$	$2.4121285878219143 \times 10^{-13}$
606	$2.4526878533919132 \times 10^{-13}$	$2.4539825450821287 \times 10^{-13}$
1320	$2.6438002312311335 \times 10^{-13}$	$2.6434075061581286 \times 10^{-13}$
607	$2.7564632155360420 \times 10^{-13}$	$2.7587419394270576 \times 10^{-13}$
673	$3.3216321735777106 \times 10^{-13}$	$3.3292699520223907 \times 10^{-13}$
1847	$3.7053462655372513 \times 10^{-13}$	$3.7054904221588347 \times 10^{-13}$
1106	$3.7152143682759933 \times 10^{-13}$	$3.7304937173052122 \times 10^{-13}$
836	$3.7152165146427532 \times 10^{-13}$	$3.7305614585941771 \times 10^{-13}$
1139	$4.2903433434223590 \times 10^{-13}$	$4.2982311412160188 \times 10^{-13}$
1111	$4.6024786593854277 \times 10^{-13}$	$4.6012083161411539 \times 10^{-13}$
1983	$4.7537858949137650 \times 10^{-13}$	$4.7623066288861482 \times 10^{-13}$
1982	$4.7537858949137659 \times 10^{-13}$	$4.7623066288861420 \times 10^{-13}$
1206	$4.9005383980819879 \times 10^{-13}$	$4.9103996487898494 \times 10^{-13}$
1248	$5.4215261041052969 \times 10^{-13}$	$5.4206633576862950 \times 10^{-13}$
1389	$5.6952386105857560 \times 10^{-13}$	$5.7069039933140155 \times 10^{-13}$
2316	$5.7787995102879037 \times 10^{-13}$	$5.7778485086388285 \times 10^{-13}$
2251	$5.8451056453053942 \times 10^{-13}$	$5.8560703149866677 \times 10^{-13}$
1550	$5.9419744640673624 \times 10^{-13}$	$5.9423478662861964 \times 10^{-13}$
1467	$5.9547992913572827 \times 10^{-13}$	$5.9840571191680834 \times 10^{-13}$
1210	$6.2950937697950682 \times 10^{-13}$	$6.3093930565636525 \times 10^{-13}$
672	$6.7750281230027234 \times 10^{-13}$	$6.7888055816196768 \times 10^{-13}$
2535	$6.7994609253976490 \times 10^{-13}$	$6.8019177743560597 \times 10^{-13}$
1386	$6.9022141200314815 \times 10^{-13}$	$6.9182522619386964 \times 10^{-13}$
1500	$6.9949994847515011 \times 10^{-13}$	$6.9941320238236315 \times 10^{-13}$
1868	$7.0801168671166455 \times 10^{-13}$	$7.0857850200343826 \times 10^{-13}$
2534	$7.1587558562101137 \times 10^{-13}$	$7.1579114736956146 \times 10^{-13}$

Table 9: Reactions with non-physical time scales from individual analysis

		Forward Coefficients			Reverse Coefficients		
#	Reaction	a_j $[cm^3/(mol\ s\ K^\beta)]$	β_j	$\overline{E}_j$ $[cal/mol]$	a_j $[cm^3/(mol\ s\ K^\beta)]$	β_j	$\overline{E}_j$ $[cal/mol]$
606	$ic3h7o \rightleftharpoons ch3coch3 + h$	2.000×10^{14}	0.00	2.150×10^4	7.888×10^{12}	0.25	6.810×10^3
607	$nc3h7o \rightleftharpoons c2h5cho + h$	2.510×10^{14}	0.00	2.340×10^4	4.149×10^9	1.14	4.470×10^3
609	$nc3h7o2h \rightleftharpoons nc3h7o + oh$	1.500×10^{16}	0.00	4.250×10^4	1.744×10^8	1.72	-3.025×10^3
610	$ic3h7o2h \rightleftharpoons ic3h7o + oh$	9.450×10^{15}	0.00	4.160×10^4	1.362×10^8	1.69	-4.185×10^3
672	$nc3h7o2 \rightleftharpoons nc3h7 + o2$	3.364×10^{19}	-1.32	3.576×10^4	4.520×10^{12}	0.00	0.00
673	$ic3h7o2 \rightleftharpoons ic3h7 + o2$	2.803×10^{17}	-0.62	3.604×10^4	7.540×10^{12}	0.00	0.00
718	$c4h7o \rightleftharpoons ch3cho + c2h3$	7.940×10^{14}	0.00	1.900×10^4	1.000×10^{10}	0.00	2.000×10^4
719	$c4h7o \rightleftharpoons c2h3cho + ch3$	7.940×10^{14}	0.00	1.900×10^4	1.000×10^{10}	0.00	2.000×10^4
725	$c4h8oh-1o2 \rightleftharpoons c4h8oh-1 + o2$	1.829×10^{18}	0.15	4.747×10^4	2.000×10^{12}	0.00	0.00
726	$c4h8oh-2o2 \rightleftharpoons c4h8oh-2 + o2$	4.092×10^{19}	-0.18	5.198×10^4	2.000×10^{12}	0.00	0.00
727	$c4h8oh-1o2 \rightleftharpoons c2h5cho + ch2o + oh$	1.000×10^{16}	0.00	2.500×10^4	0.00	0.00	0.00
728	$c4h8oh-2o2 \rightleftharpoons oh + ch3cho + ch3cho$	1.000×10^{16}	0.00	2.500×10^4	0.00	0.00	0.00
777	$ic4h8ooh-to2 \rightleftharpoons ic4h8o2h-t + o2$	2.266×10^{27}	-3.23	3.964×10^4	1.410×10^{13}	0.00	0.00
830	$ic4h9o \rightleftharpoons ch2o + ic3h7$	2.000×10^{14}	0.00	1.750×10^4	2.157×10^{11}	0.11	1.151×10^4
831	$tc4h9o \rightleftharpoons ch3coch3 + ch3$	4.865×10^{14}	-0.25	1.524×10^4	1.500×10^{11}	0.00	1.190×10^4
834	$pc4h9o2h \rightleftharpoons pc4h9o + oh$	1.500×10^{16}	0.00	4.250×10^4	1.449×10^8	1.74	-3.055×10^3
835	$sc4h9o2h \rightleftharpoons sc4h9o + oh$	9.450×10^{15}	0.00	4.160×10^4	1.205×10^8	1.70	-4.215×10^3
836	$tc4h9o2h \rightleftharpoons tc4h9o + oh$	5.950×10^{15}	0.00	4.254×10^4	2.954×10^7	1.72	-2.185×10^3
837	$ic4h9o2h \rightleftharpoons ic4h9o + oh$	1.500×10^{16}	0.00	4.250×10^4	1.663×10^8	1.72	-3.245×10^3
1018	$ch3coch2o2h \rightleftharpoons ch3coch2o + oh$	1.000×10^{16}	0.00	4.300×10^4	2.038×10^9	1.55	-4.375×10^3
1055	$bc5h11o2 \rightleftharpoons bc5h11 + o2$	2.323×10^{24}	-2.50	3.818×10^4	1.410×10^{13}	0.00	0.00
1105	$ac5h11o2h \rightleftharpoons ac5h11o + oh$	1.500×10^{16}	0.00	4.250×10^4	1.566×10^8	1.73	-3.035×10^3
1106	$bc5h11o2h \rightleftharpoons bc5h11o + oh$	5.950×10^{15}	0.00	4.254×10^4	3.783×10^7	1.74	-2.205×10^3
1107	$cc5h11o2h \rightleftharpoons cc5h11o + oh$	9.450×10^{15}	0.00	4.160×10^4	9.537×10^7	1.74	-4.225×10^3
1108	$dc5h11o2h \rightleftharpoons dc5h11o + oh$	1.500×10^{16}	0.00	4.250×10^4	1.566×10^8	1.73	-3.035×10^3
1110	$bc5h11o \rightleftharpoons c2h5 + ch3coch3$	9.831×10^{17}	-1.16	1.616×10^4	8.500×10^{10}	0.00	1.190×10^4
1111	$cc5h11o \rightleftharpoons ch3cho + ic3h7$	5.480×10^{18}	-1.43	1.878×10^4	7.500×10^{10}	0.00	1.190×10^4
1138	$ac5h10ooh-bo2 \rightleftharpoons ac5h10ooh-b + o2$	4.734×10^{27}	-3.24	3.964×10^4	1.410×10^{13}	0.00	0.00
1139	$ac5h10ooh-co2 \rightleftharpoons ac5h10ooh-c + o2$	1.374×10^{23}	-2.26	3.799×10^4	7.540×10^{12}	0.00	0.00
1145	$cc5h10ooh-bo2 \rightleftharpoons cc5h10ooh-b + o2$	1.568×10^{24}	-2.43	3.744×10^4	1.410×10^{13}	0.00	0.00
1148	$dc5h10ooh-bo2 \rightleftharpoons dc5h10ooh-b + o2$	2.107×10^{24}	-2.48	3.745×10^4	1.410×10^{13}	0.00	0.00
1206	$c5h11o2-1 \rightleftharpoons c5h11-1 + o2$	1.956×10^{20}	-1.50	3.581×10^4	4.520×10^{12}	0.00	0.00
1210	$c5h11o2-2 \rightleftharpoons c5h11-2 + o2$	5.194×10^{17}	-0.78	3.597×10^4	7.540×10^{12}	0.00	0.00
1243	$c5h11o2h-1 \rightleftharpoons c5h11o-1 + oh$	1.500×10^{16}	0.00	4.250×10^4	1.406×10^8	1.75	-3.055×10^3
1244	$c5h11o2h-2 \rightleftharpoons c5h11o-2 + oh$	9.450×10^{15}	0.00	4.160×10^4	6.741×10^7	1.78	-4.285×10^3

Table 9 – continued from previous page

		Forward Coefficients			Reverse Coefficients		
#	Reaction	a_j $[(mol/cm^3)^{(1-\sum_{i=1}^{N}\nu'_{ij})}/s/K^{\beta_j}]$	β_j	$\overline{E}_j$ $[cal/mol]$	a_j $[(mol/cm^3)^{(1-\sum_{i=1}^{N}\nu'_{ij})}/s/K^{\beta_j}]$	β_j	$\overline{E}_j$ $[cal/mol]$
1245	$c5h11o2h\text{-}3 \rightleftharpoons c5h11o\text{-}3 + oh$	9.450×10^{15}	0.00	4.160×10^4	1.344×10^8	1.78	-4.285×10^3
1248	$c5h11o\text{-}3 \rightleftharpoons c2h5 + c2h5cho$	2.282×10^{21}	-2.18	2.015×10^4	8.500×10^{10}	0.00	1.190×10^4
1319	$neoc5h11o2h \rightleftharpoons neoc5h11o + oh$	1.500×10^{16}	0.00	4.250×10^4	1.386×10^8	1.75	-3.055×10^3
1320	$neoc5h11o \rightleftharpoons ch2o + tc4h9$	1.349×10^{22}	-2.34	1.899×10^4	2.000×10^{11}	0.00	1.190×10^4
1386	$sc4h9o2 \rightleftharpoons sc4h9 + o2$	2.056×10^{17}	-0.68	3.574×10^4	7.540×10^{12}	0.00	0.00
1389	$pc4h9o2 \rightleftharpoons pc4h9 + o2$	6.155×10^{19}	-1.38	3.551×10^4	4.520×10^{12}	0.00	0.00
1392	$tc4h9o2 \rightleftharpoons tc4h9 + o2$	4.897×10^{24}	-2.51	3.746×10^4	1.410×10^{13}	0.00	0.00
1398	$c2h3o1\text{-}2 \rightleftharpoons ch3co$	8.500×10^{14}	0.00	1.400×10^4	1.488×10^{14}	-0.01	4.768×10^4
1399	$c2h3o1\text{-}2 \rightleftharpoons ch2cho$	1.000×10^{14}	0.00	1.400×10^4	1.615×10^{15}	-0.41	4.246×10^4
1402	$c3ket12 \rightleftharpoons ch3cho + hco + oh$	1.050×10^{16}	0.00	4.160×10^4	0.00	0.00	0.00
1403	$c3ket13 \rightleftharpoons ch2o + ch2cho + oh$	1.500×10^{16}	0.00	4.200×10^4	0.00	0.00	0.00
1404	$c3ket21 \rightleftharpoons ch2o + ch3co + oh$	1.500×10^{16}	0.00	4.200×10^4	0.00	0.00	0.00
1405	$nc4ket12 \rightleftharpoons c2h5cho + hco + oh$	1.050×10^{16}	0.00	4.160×10^4	0.00	0.00	0.00
1406	$nc4ket13 \rightleftharpoons ch3cho + ch2cho + oh$	1.050×10^{16}	0.00	4.160×10^4	0.00	0.00	0.00
1407	$nc4ket14 \rightleftharpoons ch2ch2cho + ch2o + oh$	1.500×10^{16}	0.00	4.200×10^4	0.00	0.00	0.00
1408	$nc4ket21 \rightleftharpoons ch2o + c2h5co + oh$	1.500×10^{16}	0.00	4.200×10^4	0.00	0.00	0.00
1409	$nc4ket23 \rightleftharpoons ch3cho + ch3co + oh$	1.050×10^{16}	0.00	4.160×10^4	0.00	0.00	0.00
1410	$nc4ket24 \rightleftharpoons ch2o + ch3coch2 + oh$	1.500×10^{16}	0.00	4.200×10^4	0.00	0.00	0.00
1411	$ic4ketii \rightleftharpoons ch2o + c2h5co + oh$	1.500×10^{16}	0.00	4.200×10^4	0.00	0.00	0.00
1412	$ic4ketit \rightleftharpoons ch3coch3 + hco + oh$	9.500×10^{15}	0.00	4.254×10^4	0.00	0.00	0.00
1413	$nc5ket12 \rightleftharpoons nc3h7cho + hco + oh$	1.050×10^{16}	0.00	4.160×10^4	0.00	0.00	0.00
1414	$nc5ket13 \rightleftharpoons c2h5cho + ch2cho + oh$	1.050×10^{16}	0.00	4.160×10^4	0.00	0.00	0.00
1415	$nc5ket14 \rightleftharpoons ch3cho + ch2ch2cho + oh$	1.050×10^{16}	0.00	4.160×10^4	0.00	0.00	0.00
1416	$nc5ket15 \rightleftharpoons ch2o + c3h6cho\text{-}1 + oh$	1.500×10^{16}	0.00	4.200×10^4	0.00	0.00	0.00
1417	$nc5ket21 \rightleftharpoons ch2o + nc3h7co + oh$	1.500×10^{16}	0.00	4.200×10^4	0.00	0.00	0.00
1418	$nc5ket23 \rightleftharpoons c2h5cho + ch3co + oh$	1.500×10^{16}	0.00	4.200×10^4	0.00	0.00	0.00
1419	$nc5ket24 \rightleftharpoons ch3cho + ch3coch2 + oh$	1.500×10^{16}	0.00	4.200×10^4	0.00	0.00	0.00
1420	$nc5ket25 \rightleftharpoons ch2o + ch2ch2coch3 + oh$	1.500×10^{16}	0.00	4.200×10^4	0.00	0.00	0.00
1421	$nc5ket31 \rightleftharpoons ch2o + c2h5coch2 + oh$	1.500×10^{16}	0.00	4.200×10^4	0.00	0.00	0.00
1422	$nc5ket32 \rightleftharpoons ch3cho + c2h5co + oh$	1.050×10^{16}	0.00	4.160×10^4	0.00	0.00	0.00
1423	$ic5ketaa \rightleftharpoons ch2o + c3h6cho\text{-}3 + oh$	1.500×10^{16}	0.00	4.200×10^4	0.00	0.00	0.00
1424	$ic5ketab \rightleftharpoons c2h5coch3 + hco + oh$	9.500×10^{15}	0.00	4.254×10^4	0.00	0.00	0.00
1425	$ic5ketac \rightleftharpoons ch3cho + ch3chcho + oh$	1.050×10^{16}	0.00	4.160×10^4	0.00	0.00	0.00
1426	$ic5ketad \rightleftharpoons ch2o + ic3h6cho + oh$	1.500×10^{16}	0.00	4.200×10^4	0.00	0.00	0.00
1427	$ic5ketca \rightleftharpoons ch2o + ch3chcoch3 + oh$	1.500×10^{16}	0.00	4.200×10^4	0.00	0.00	0.00
1428	$ic5ketcb \rightleftharpoons ch3coch3 + ch3co + oh$	9.500×10^{15}	0.00	4.254×10^4	0.00	0.00	0.00

Continued on next page

Table 9 – continued from previous page

#	Reaction	Forward Coefficients			Reverse Coefficients		
		a_j $[(mol/cm^3)^{(1-\sum_{i=1}^{N}\nu'_{ij})}/s/K^{\beta_j}]$	β_j	$\overline{E}_j$ $[cal/mol]$	a_j $[(mol/cm^3)^{(1-\sum_{i=1}^{N}\nu'_{ij})}/s/K^{\beta_j}]$	β_j	$\overline{E}_j$ $[cal/mol]$
1429	$ic5ketcd \rightleftharpoons ch2o + ic3h7co + oh$	$1.500{\times}10^{16}$	0.00	$4.200{\times}10^4$	0.00	0.00	0.00
1430	$ic5ketda \rightleftharpoons ch2o + c3h6cho\text{-}2 + oh$	$1.500{\times}10^{16}$	0.00	$4.200{\times}10^4$	0.00	0.00	0.00
1431	$ic5ketdb \rightleftharpoons ch3coch3 + ch2cho + oh$	$9.500{\times}10^{15}$	0.00	$4.254{\times}10^4$	0.00	0.00	0.00
1432	$ic5ketdc \rightleftharpoons ic3h7cho + hco + oh$	$1.050{\times}10^{16}$	0.00	$4.160{\times}10^4$	0.00	0.00	0.00
1433	$neoc5ket \rightleftharpoons neoc5ketox + oh$	$1.500{\times}10^{16}$	0.00	$4.200{\times}10^4$	$1.528{\times}10^8$	1.73	$-3.765{\times}10^3$
1461	$tc3h6ocho \rightleftharpoons ch3coch3 + hco$	$3.980{\times}10^{13}$	0.00	$9.700{\times}10^3$	$2.173{\times}10^8$	0.80	$1.424{\times}10^4$
1467	$ic4h7ooh \rightleftharpoons ic4h7o + oh$	$6.400{\times}10^{15}$	0.00	$4.555{\times}10^4$	$1.000{\times}10^{13}$	0.00	0.00
1487	$tc3h6o2hco \rightleftharpoons ch3coch3 + co + oh$	$4.244{\times}10^{18}$	-1.43	$4.800{\times}10^3$	0.00	0.00	0.00
1490	$ic4h9o \rightleftharpoons ic3h7cho + h$	$4.000{\times}10^{14}$	0.00	$2.150{\times}10^4$	$1.139{\times}10^{10}$	1.08	$2.500{\times}10^3$
1500	$ic3h7co \rightleftharpoons ic3h7 + co$	$1.426{\times}10^{13}$	-0.04	$1.095{\times}10^4$	$1.500{\times}10^{11}$	0.00	$4.810{\times}10^3$
1550	$o2hc4h8co \rightleftharpoons ic4h8o2h\text{-}t + co$	$3.299{\times}10^{22}$	-2.72	$1.176{\times}10^4$	$1.500{\times}10^{11}$	0.00	$4.809{\times}10^3$
1633	$ch3chocho \rightleftharpoons ch3cho + hco$	$3.980{\times}10^{13}$	0.00	$9.700{\times}10^3$	$4.335{\times}10^5$	1.72	$8.282{\times}10^3$
1647	$sc3h5co \rightleftharpoons c3h5\text{-}s + co$	$8.600{\times}10^{15}$	0.00	$2.300{\times}10^4$	$1.000{\times}10^{11}$	0.00	$6.000{\times}10^3$
1705	$pc2h4coc2h3 \rightleftharpoons c2h3co + c2h4$	$5.263{\times}10^{14}$	0.38	$2.146{\times}10^4$	$8.000{\times}10^{10}$	0.00	$1.130{\times}10^4$
1847	$neoc5kejol \rightleftharpoons ic4h8oh + co$	$2.273{\times}10^{21}$	-2.34	$1.102{\times}10^4$	$1.250{\times}10^{11}$	0.00	$4.800{\times}10^3$
1849	$neoc5h9q2 \rightleftharpoons ic4h7ooh + ch2o + oh$	$3.417{\times}10^{14}$	0.37	$3.092{\times}10^4$	0.00	0.00	0.00
1851	$neoc5h9q2\text{-}n \rightleftharpoons neoc5ket + oh$	$9.000{\times}10^{14}$	0.00	$1.500{\times}10^3$	$1.668{\times}10^9$	1.58	$3.188{\times}10^4$
1868	$hoch2o \rightleftharpoons ch2o + oh$	$1.643{\times}10^{14}$	-0.10	$2.189{\times}10^4$	$2.600{\times}10^{12}$	0.00	$-6.140{\times}10^2$
1869	$hoch2o \rightleftharpoons hocho + h$	$1.000{\times}10^{14}$	0.00	$1.490{\times}10^4$	$3.077{\times}10^{11}$	0.64	$7.944{\times}10^3$
1982	$c6h13o2\text{-}2 \rightleftharpoons c6h13\text{-}2 + o2$	$2.180{\times}10^{23}$	-2.33	$3.804{\times}10^4$	$7.540{\times}10^{12}$	0.00	0.00
1983	$c6h13o2\text{-}3 \rightleftharpoons c6h13\text{-}3 + o2$	$2.180{\times}10^{23}$	-2.33	$3.804{\times}10^4$	$7.540{\times}10^{12}$	0.00	0.00
2022	$c6h13o2h\text{-}1 \rightleftharpoons c6h13o\text{-}1 + oh$	$1.500{\times}10^{16}$	0.00	$4.250{\times}10^4$	$1.460{\times}10^8$	1.74	$-3.045{\times}10^3$
2023	$c6h13o2h\text{-}2 \rightleftharpoons c6h13o\text{-}2 + oh$	$1.250{\times}10^{16}$	0.00	$4.160{\times}10^4$	$3.589{\times}10^7$	1.81	$-4.325{\times}10^3$
2024	$c6h13o2h\text{-}3 \rightleftharpoons c6h13o\text{-}3 + oh$	$1.250{\times}10^{16}$	0.00	$4.160{\times}10^4$	$3.589{\times}10^7$	1.81	$-4.325{\times}10^3$
2079	$nc6ket12 \rightleftharpoons nc4h9cho + hco + oh$	$1.050{\times}10^{16}$	0.00	$4.160{\times}10^4$	0.00	0.00	0.00
2080	$nc6ket13 \rightleftharpoons nc3h7cho + ch2cho + oh$	$1.050{\times}10^{16}$	0.00	$4.160{\times}10^4$	0.00	0.00	0.00
2081	$nc6ket14 \rightleftharpoons c2h5cho + ch2ch2cho + oh$	$1.050{\times}10^{16}$	0.00	$4.160{\times}10^4$	0.00	0.00	0.00
2082	$nc6ket15 \rightleftharpoons ch3cho + c3h6cho\text{-}1 + oh$	$1.050{\times}10^{16}$	0.00	$4.160{\times}10^4$	0.00	0.00	0.00
2083	$nc6ket21 \rightleftharpoons ch2o + nc4h9co + oh$	$1.500{\times}10^{16}$	0.00	$4.200{\times}10^4$	0.00	0.00	0.00
2084	$nc6ket23 \rightleftharpoons nc3h7cho + ch3co + oh$	$1.050{\times}10^{16}$	0.00	$4.160{\times}10^4$	0.00	0.00	0.00
2085	$nc6ket24 \rightleftharpoons c2h5cho + ch3coch2 + oh$	$1.050{\times}10^{16}$	0.00	$4.160{\times}10^4$	0.00	0.00	0.00
2086	$nc6ket25 \rightleftharpoons ch3cho + ch2ch2coch3 + oh$	$1.050{\times}10^{16}$	0.00	$4.160{\times}10^4$	0.00	0.00	0.00
2087	$nc6ket26 \rightleftharpoons ch2o + c3h6coch3\text{-}1 + oh$	$1.500{\times}10^{16}$	0.00	$4.200{\times}10^4$	0.00	0.00	0.00
2088	$nc6ket31 \rightleftharpoons ch2o + nc3h7coch2 + oh$	$1.500{\times}10^{16}$	0.00	$4.200{\times}10^4$	0.00	0.00	0.00
2089	$nc6ket32 \rightleftharpoons ch3cho + nc3h7co + oh$	$1.050{\times}10^{16}$	0.00	$4.160{\times}10^4$	0.00	0.00	0.00
2090	$nc6ket34 \rightleftharpoons c2h5cho + c2h5co + oh$	$1.050{\times}10^{16}$	0.00	$4.160{\times}10^4$	0.00	0.00	0.00

Table 9 – continued from previous page

		Forward Coefficients			Reverse Coefficients		
#	Reaction	a_j $[(mol/cm^3)^{(1-\sum_{i=1}^{N}\nu'_{ij})}/s/K^{\beta_j}]$	β_j	$\overline{E}_j$ $[cal/mol]$	a_j $[(mol/cm^3)^{(1-\sum_{i=1}^{N}\nu'_{ij})}/s/K^{\beta_j}]$	β_j	$\overline{E}_j$ $[cal/mol]$
2091	$nc6ket35 \rightleftharpoons ch3cho + c2h5coch2 + oh$	1.050×10^{16}	0.00	4.160×10^4	0.00	0.00	0.00
2092	$nc6ket36 \rightleftharpoons ch2o + c2h5coc2h4p + oh$	1.500×10^{16}	0.00	4.200×10^4	0.00	0.00	0.00
2251	$c7h15o2\text{-}3 \rightleftharpoons c7h15\text{-}3 + o2$	9.879×10^{21}	-1.97	3.786×10^4	7.540×10^{12}	0.00	0.00
2309	$c7h15o2h\text{-}1 \rightleftharpoons c7h15o\text{-}1 + oh$	1.500×10^{16}	0.00	4.250×10^4	1.434×10^8	1.74	-3.055×10^3
2310	$c7h15o2h\text{-}2 \rightleftharpoons c7h15o\text{-}2 + oh$	1.250×10^{16}	0.00	4.160×10^4	5.715×10^7	1.84	-4.355×10^3
2311	$c7h15o2h\text{-}3 \rightleftharpoons c7h15o\text{-}3 + oh$	1.250×10^{16}	0.00	4.160×10^4	9.507×10^8	1.42	-4.525×10^3
2312	$c7h15o2h\text{-}4 \rightleftharpoons c7h15o\text{-}4 + oh$	1.250×10^{16}	0.00	4.160×10^4	5.715×10^7	1.84	-4.355×10^3
2316	$c7h15o\text{-}4 \rightleftharpoons nc3h7cho + nc3h7$	6.684×10^{21}	-2.29	2.162×10^4	1.000×10^{11}	0.00	1.290×10^4
2382	$nc7ket12 \rightleftharpoons nc5h11cho + hco + oh$	1.050×10^{16}	0.00	4.160×10^4	0.00	0.00	0.00
2383	$nc7ket13 \rightleftharpoons nc4h9cho + ch2cho + oh$	1.050×10^{16}	0.00	4.160×10^4	0.00	0.00	0.00
2384	$nc7ket14 \rightleftharpoons nc3h7cho + ch2ch2cho + oh$	1.050×10^{16}	0.00	4.160×10^4	0.00	0.00	0.00
2385	$nc7ket15 \rightleftharpoons c2h5cho + c3h6cho\text{-}1 + oh$	1.050×10^{16}	0.00	4.160×10^4	0.00	0.00	0.00
2386	$nc7ket21 \rightleftharpoons ch2o + nc5h11co + oh$	1.500×10^{16}	0.00	4.200×10^4	0.00	0.00	0.00
2387	$nc7ket23 \rightleftharpoons nc4h9cho + ch3co + oh$	1.050×10^{16}	0.00	4.160×10^4	0.00	0.00	0.00
2388	$nc7ket24 \rightleftharpoons nc3h7cho + ch3coch2 + oh$	1.050×10^{16}	0.00	4.160×10^4	0.00	0.00	0.00
2389	$nc7ket25 \rightleftharpoons c2h5cho + ch2ch2coch3 + oh$	1.050×10^{16}	0.00	4.160×10^4	0.00	0.00	0.00
2390	$nc7ket26 \rightleftharpoons ch3cho + c3h6coch3\text{-}1 + oh$	1.050×10^{16}	0.00	4.160×10^4	0.00	0.00	0.00
2391	$nc7ket31 \rightleftharpoons ch2o + nc4h9coch2 + oh$	1.500×10^{16}	0.00	4.200×10^4	0.00	0.00	0.00
2392	$nc7ket32 \rightleftharpoons ch3cho + nc4h9co + oh$	1.050×10^{16}	0.00	4.160×10^4	0.00	0.00	0.00
2393	$nc7ket34 \rightleftharpoons nc3h7cho + c2h5co + oh$	1.050×10^{16}	0.00	4.160×10^4	0.00	0.00	0.00
2394	$nc7ket35 \rightleftharpoons c2h5cho + c2h5coch2 + oh$	1.050×10^{16}	0.00	4.160×10^4	0.00	0.00	0.00
2395	$nc7ket36 \rightleftharpoons ch3cho + c2h5coc2h4p + oh$	1.050×10^{16}	0.00	4.160×10^4	0.00	0.00	0.00
2396	$nc7ket37 \rightleftharpoons ch2o + c3h6coc2h5\text{-}1 + oh$	1.500×10^{16}	0.00	4.200×10^4	0.00	0.00	0.00
2397	$nc7ket41 \rightleftharpoons ch2o + nc3h7coc2h4p + oh$	1.500×10^{16}	0.00	4.200×10^4	0.00	0.00	0.00
2398	$nc7ket42 \rightleftharpoons ch3cho + nc3h7coch2 + oh$	1.050×10^{16}	0.00	4.160×10^4	0.00	0.00	0.00
2399	$nc7ket43 \rightleftharpoons c2h5cho + nc3h7co + oh$	1.050×10^{16}	0.00	4.160×10^4	0.00	0.00	0.00
2534	$c6h11o1\text{-}4 \rightleftharpoons ac3h5cho + c2h5$	7.268×10^{20}	-2.10	1.887×10^4	1.000×10^{11}	0.00	9.600×10^3
2535	$c6h11o1\text{-}4 \rightleftharpoons c2h5cho + c3h5\text{-}a$	1.211×10^{21}	-2.46	5.641×10^3	5.000×10^{10}	0.00	9.600×10^3